Identification of multiple transcription factor genes potentially involved in the development of electrosensory versus mechanosensory lateral line organs

Martin Minařík[1], Melinda S. Modrell[1], J. Andrew Gillis[2,3], Alexander S. Campbell[1], Isobel Fuller[1], Rachel Lyne[5], Gos Micklem[5], David Gela[4], Martin Pšenička[4] and Clare V. H. Baker[1]*

[1]Department of Physiology, Development & Neuroscience, University of Cambridge, Cambridge, UK
[2]Department of Zoology, University of Cambridge, Cambridge, UK
[3]Marine Biological Laboratory, 7 MBL Street, Woods Hole, MA 02543, USA
[4]Faculty of Fisheries and Protection of Waters, Research Institute of Fish Culture and Hydrobiology, University of South Bohemia in České Budějovice, Vodňany, Czech Republic
[5]Department of Genetics, University of Cambridge, Cambridge, UK
*For correspondence: cvhb1@cam.ac.uk

Abstract

In electroreceptive jawed vertebrates, embryonic lateral line placodes give rise to electrosensory ampullary organs as well as mechanosensory neuromasts. Previous reports of shared gene expression suggest that conserved mechanisms underlie electroreceptor and mechanosensory hair cell development and that electroreceptors evolved as a transcriptionally related 'sister cell type' to hair cells. We previously identified only one transcription factor gene, *Neurod4*, as ampullary organ-restricted in the developing lateral line system of a chondrostean ray-finned fish, the Mississippi paddlefish (*Polyodon spathula*). The other 16 transcription factor genes we previously validated in paddlefish were expressed in both ampullary organs and neuromasts. Here, we used our published lateral line organ-enriched gene-set (arising from differential bulk RNA-seq in late-larval paddlefish), together with a candidate gene approach, to identify 23 transcription factor genes expressed in the developing lateral line system of a more experimentally tractable chondrostean, the sterlet (*Acipenser ruthenus*, a small sturgeon), and/or that of paddlefish. Twelve are expressed in both ampullary organs and neuromasts, consistent with conservation of molecular mechanisms. Six are novel electrosensory-restricted transcription factor genes *(Irx5*, *Satb2*, *Insm1*, *Sp5*, *MafA* and *Rorc*), and five are the first-reported mechanosensory-restricted transcription factor genes (*Foxg1*, *Sox8*, *Isl1*, *Hmx2* and *Rorb*). However, as previously reported, *Sox8* is expressed in ampullary organs as well as neuromasts in a shark (*Scyliorhinus canicula*), suggesting the existence of lineage-specific differences between cartilaginous and ray-finned fishes. Overall, our results support the hypothesis that ampullary organs and neuromasts develop via largely conserved transcriptional mechanisms, and identify multiple transcription factors potentially involved in the formation of electrosensory versus mechanosensory lateral line organs.

Introduction

In jawed anamniotes, mechanosensory hair cells are found in the inner ear, in the spiracular organ associated with the first pharyngeal cleft (lost in amphibians, bichirs and teleosts; see Norris and Hughes, 1920; von Bartheld and Giannessi, 2011), and in lateral line neuromasts: small sense organs distributed in lines over the head and trunk, which respond to local water movement (see e.g., Mogdans, 2019; Webb, 2021). In electroreceptive species (e.g., cartilaginous fishes, ray-finned fishes including the chondrostean paddlefishes and sturgeons, and urodele amphibians like the axolotl), the lateral line system includes electrosensory ampullary organs containing supporting cells and electroreceptors that detect weak electric fields, primarily for hunting or avoiding predators (see e.g., Crampton, 2019; Leitch and Julius, 2019; Chagnaud et al., 2021).

Like hair cells, electroreceptors have an apical primary cilium (lost during maturation in cochlear hair cells; Lu and Sipe, 2016) and basolateral ribbon synapses with afferent nerve terminals (Jørgensen, 2005; Baker, 2019). However, electroreceptors lack the apical hair bundle (staircase array of microvilli) where mechanoelectrical transduction occurs (Ó Maoiléidigh and Ricci, 2019; Caprara and Peng, 2022). The main anamniote developmental models - the teleost zebrafish and the frog *Xenopus* - lack ampullary organs: electroreception was lost in the ray-finned bony fish radiation leading to teleosts, and in the lobe-finned bony amphibian lineage leading to frogs (Baker et al., 2013; Baker, 2019; Crampton, 2019). (Physiologically distinct lateral line electroreceptors evolved independently in some teleost lineages; see e.g., Baker et al., 2013; Baker, 2019; Crampton, 2019.)

Neuromasts and ampullary organs, together with the neurons in lateral line ganglia that provide their afferent innervation, develop from a series of cranial lateral line placodes (Northcutt, 1997; Baker et al., 2013; Piotrowski and Baker, 2014). These either elongate to form sensory ridges that fragment, with a line of neuromasts forming first in the ridge's centre and ampullary organs (if present) forming later on the ridge's flanks (Northcutt, 1997; Piotrowski and Baker, 2014). Alternatively, as in the ray-finned bony teleost zebrafish, lateral line primordia migrate as cell collectives, depositing neuromasts in their wake (Piotrowski and Baker, 2014). The lateral line placode origin of ampullary organs was first shown by grafting and ablation in a lobe-finned bony tetrapod, the axolotl (Northcutt et al., 1995). Our DiI-labelling studies in a chondrostean ray-finned fish (Mississippi paddlefish, *Polyodon spathula*) (Modrell et al., 2011a) and a cartilaginous fish (little skate, *Leucoraja erinacea*) (Gillis et al., 2012) showed that individual elongating lateral line placodes form ampullary organs and neuromasts across all non-teleost jawed vertebrates (reviewed in Baker et al., 2013).

What molecular mechanisms underlie the formation of ampullary organs versus neuromasts within the same lateral line sensory ridge? We have identified a range of ampullary organ-expressed genes in different electroreceptive vertebrates using a candidate gene approach (O'Neill et al., 2007; Modrell et al., 2011a; Modrell et al., 2011b; Gillis et al., 2012; Modrell and Baker, 2012; Modrell et al., 2017a; Modrell et al., 2017b). More recently, we took an unbiased differential RNA-seq approach, comparing the transcriptome of late-larval paddlefish gill-flaps (covered in ampullary organs, plus some neuromasts) versus fins (no lateral line organs) (Modrell et al., 2017a). The resultant lateral line organ-enriched dataset of around 500 genes (Modrell et al., 2017a) is not exhaustive: it includes most, but not all, of the genes identified in paddlefish ampullary organs via the candidate gene approach (Modrell et al., 2011a; Modrell et al., 2011b; Modrell et al., 2017a; Modrell et al., 2017b). *In situ* hybridization for selected candidate genes from this dataset suggested that electroreceptors and hair cells are closely related, e.g., late-larval ampullary organs express genes encoding proteins essential for neurotransmission specifically at hair-cell (but not photoreceptor) ribbon synapses in the basolateral cell membrane (Pangrsic et al., 2018; Moser et al., 2020), such as vGlut3, otoferlin and $Ca_v1.3$ (Modrell et al., 2017a). $Ca_v1.3$ has also been identified as the electrosensitive voltage-gated Ca^{2+} channel in the apical electroreceptor membrane (Bennett and Obara, 1986; Bodznick and Montgomery, 2005) in shark and skate species (i.e., in cartilaginous fishes) (Bellono et al., 2017; Bellono et al., 2018).

Developing ampullary organs also express key 'hair cell' transcription factor genes including *Atoh1*, *Pou4f3* (*Brn3c*) and *Six1* (Modrell et al., 2011a; Butts et al., 2014; Modrell et al., 2017a). These are critical for hair cell formation and, in combination with *Gfi1*, can drive an immature 'hair cell-like' fate in mouse embryonic stem cells, adult cochlear supporting cells and fibroblasts (see Roccio et al., 2020; Chen et al., 2021; Iyer and Groves, 2021; Iyer et al., 2022). Co-expression of *Atoh1*, *Pou4f3* and *Gfi1* is sufficient to drive a more mature hair cell fate in postnatal cochlear supporting cells (Chen et al., 2021). The expression of *Atoh1*, *Pou4f3* and *Six1* in developing ampullary organs, as well as neuromasts, suggests that molecular mechanisms underlying electroreceptor development are likely to be highly conserved with those underlying hair cell formation (Modrell et al., 2011a; Modrell et al., 2017a). Nevertheless, hair cells and electroreceptors are morphologically and functionally distinct (Jørgensen, 2005; Baker, 2019). Validation of multiple candidate genes from the late-larval paddlefish lateral line organ-enriched dataset had identified only a handful of genes with expression in developing ampullary organs but not neuromasts (Modrell et al., 2017a). These were the basic helix-loop-helix (bHLH) transcription factor gene *Neurod4*, plus two voltage-gated potassium channel subunit genes (*Kcna5*, encoding $K_v1.5$, and *Kcnab3*, encoding the accessory subunit $K_v\beta3$) and a calcium-chelating beta-parvalbumin, all presumably involved in electroreceptor function (Modrell et al., 2017a).

In recent years, another chondrostean fish, the sterlet (a sturgeon, *Acipenser ruthenus*), has been developed as an experimentally tractable non-teleost model (see e.g., Saito and Psenicka, 2015; Chen et al., 2018; Baloch et al., 2019; Stundl et al., 2020; Du et al., 2020; Stundl et al., 2022). In contrast to the limited Mississippi paddlefish spawning season, many hundreds of sterlet embryos are available each week for up to several months in fully equipped laboratory research facilities. We have therefore turned to the sterlet as a tractable model for studying the molecular control of lateral line hair cell and electroreceptor development. In the current study, we describe lateral line hair cell and electroreceptor differentiation in the sterlet, and the expression in sterlet and/or paddlefish of almost all of the remaining transcription factor genes from the paddlefish late-larval lateral line organ-enriched dataset (Modrell et al., 2017a), plus a few additional candidates. We report expression within the developing lateral line system of 23 novel transcription factor genes. Twelve - including the key 'hair cell' transcription factor gene *Gfi1* - were expressed in both ampullary organs and neuromasts, supporting conserved molecular mechanisms. Six transcription factor genes proved to be electrosensory-restricted, while five represent the first-reported mechanosensory lateral line-restricted transcription factors. These eleven genes, plus ampullary organ-restricted *Neurod4* (Modrell et al., 2017a), are good candidates to be involved in the development of electrosensory versus mechanosensory lateral line organs.

Results

Characterizing lateral line hair cell and electroreceptor development in sterlet

In order to use the sterlet as a more experimentally tractable model for lateral line organ development than the Mississippi paddlefish (Modrell et al., 2011b; Modrell et al., 2011a; Modrell et al., 2017b; Modrell et al., 2017a), we first characterized the timing and distribution of lateral line hair cell and electroreceptor differentiation (staging according to Dettlaff et al., 1993). The development of lateral line placodes, neuromasts and ampullary organs had previously been described in the shovelnose sturgeon, *Scaphirhynchus platorynchus* (Gibbs and Northcutt, 2004a); ampullary organ formation had also been described in a sturgeon in the same genus as the sterlet, the Adriatic sturgeon, *A. naccari* (Camacho et al., 2007). In *S. platorynchus*, all lateral line placodes were present at stage 30 and had started to elongate into sensory ridges (Gibbs and Northcutt, 2004a). By the time of hatching at stage 36, neuromast primordia were present within the sensory ridges at the centre of all the lateral line placodes but only a few mature neuromasts had formed, specifically in the otic lateral line (Gibbs and Northcutt, 2004a). At stage 41, roughly midway between hatching (stage 36) and the onset of independent feeding (stage 45), ampullary organ primordia were present in the lateral zones of the anterodorsal, anteroventral, otic and supratemporal sensory ridges (Gibbs

149 and Northcutt, 2004a). At stage 45, mature ampullary organs were present in the infraorbital,
150 otic and posterior preopercular fields and ampullary organs continued to develop over the next
151 three weeks (Gibbs and Northcutt, 2004a). By stage 45 in *A. naccari*, in contrast, ampullary
152 organs are ultrastructurally mature at almost all sites and thought to be functional (Camacho
153 et al., 2007). Camacho et al. (2007) speculate that the difference is due to *S. platorynchus*
154 reaching stage 45 on day 4 post-hatching, leaving less time for completion of ampullary organ
155 development than in *A. naccari*, which reaches stage 45 on day 9 post-hatching.

156 To examine the formation and distribution of developing neuromasts and ampullary
157 organs in sterlet, we focused on the stages between stage 35, i.e., the stage before hatching
158 (stage 36), up to the onset of independent feeding at stage 45, which is reached in the sterlet
159 at 14 days post-fertilization (dpf; Zeiske et al., 2003). Figure 1 shows a temporal overview of
160 the expression by *in situ* hybridization (ISH) in sterlet of *Eya4*, an otic and lateral line
161 primordium marker that is eventually restricted to differentiated hair cells and electroreceptors
162 (Modrell and Baker, 2012; Baker et al., 2013) (Figure 1A-D) and *Sox2*, which is also expressed
163 by lateral line primordia and is eventually restricted to supporting cells in both ampullary
164 organs and neuromasts, with stronger expression in neuromasts (Modrell et al., 2017a)
165 (Figure 1E-H). (*Sox2* is also expressed in taste buds on the barbels and around the mouth;
166 Figure 1E-H.) As a marker for differentiated hair cells and electroreceptors, we used *Cacna1d*,
167 which encodes the pore-forming alpha subunit of $Ca_v1.3$ and is expressed in hair cells and
168 electroreceptors across jawed vertebrates (Modrell et al., 2017a; Bellono et al., 2017; Bellono
169 et al., 2018) (Figure 1I-L; also see Supplementary Figure S1A-H). To identify electroreceptors
170 specifically, we cloned the two voltage-gated potassium channel subunit genes that we
171 identified as electroreceptor-specific in paddlefish (Modrell et al., 2017a): *Kcnab3*, encoding
172 the accessory subunit $K_v\beta3$ (Figure 1M-P; also see Supplementary Figure S1I-P) and *Kcna5*,
173 encoding $K_v1.5$, which shows the same expression pattern as *Kcnab3* (data not shown.) The
174 earliest sign of neuromast hair cell differentiation was at stage 35 (Figure 1I; Supplementary
175 Figure S1A,B) with increasing numbers at all subsequent stages (Figure 1J-L; Supplementary
176 Figure S1C-H). Differentiated electroreceptors were not seen until stages 40-41, in some
177 ampullary organ fields (Figure 1I-K,M-O; Supplementary Figure S1I-N). By stage 45 (the onset
178 of independent feeding), all cranial neuromast lines and fields of ampullary organs with
179 differentiated electroreceptors could be identified (Figure 1D,H,L,P; Supplementary Figure
180 S1G,H,O,P). A schematic summary is shown in Figure 1Q-T.

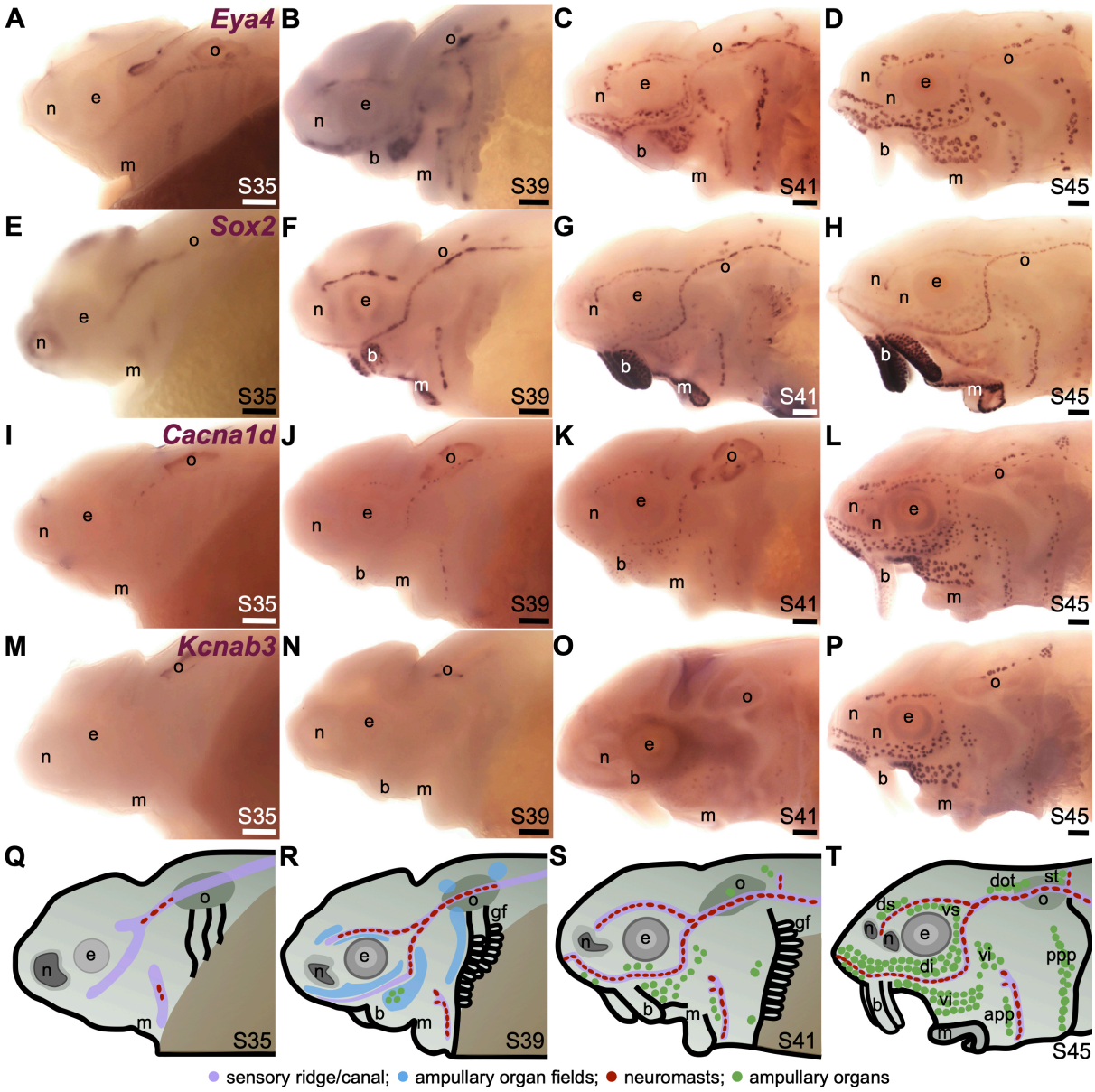

Figure 1. Time-course of neuromast and ampullary organ development in sterlet. *In situ* hybridization at selected stages in sterlet, from stage 35 (the stage before hatching occurs, at stage 36) to stage 45, the onset of independent feeding. (**A-D**) *Eya4* expression in sensory ridges and ampullary organ fields at stages 35 and 39 subsequently resolves into individual neuromasts and ampullary organs. (**E-H**) A paddlefish *Sox2* riboprobe reveals *Sox2* expression in sensory ridges at stage 35 that later resolves into a ring-like pattern in neuromasts, with weaker expression in ampullary organs from stage 41. Very strong expression is also seen in taste buds on the barbels and around the mouth. (**I-L**) Expression of *Cacna1d*, encoding the pore-forming alpha subunit of the voltage-gated calcium channel $Ca_v1.3$, reveals differentiated hair cells in a few neuromasts already at stage 35 in the otic line, near the otic vesicle, with increasing numbers later, and some differentiated electroreceptors already at stage 41. *Cacna1d* is also weakly expressed in taste buds, most clearly on the barbels. (**M-P**) Expression of electroreceptor-specific *Kcnab3* (encoding an accessory subunit for a voltage-gated K^+ channel, $K_v\beta3$) shows some differentiated electroreceptors are present by stage 41, but not earlier. (**Q-T**) Schematic representation of sterlet lateral line development at stages 35, 39, 41 and 45. Abbreviations: app, anterior preopercular ampullary organ field; b, barbels; di, dorsal infraorbital ampullary organ field; dot, dorsal otic ampullary organ field; ds, dorsal supraorbital ampullary organ field; e, eye; gf, gill filaments; m, mouth; n, naris; o, otic vesicle; ppp, posterior preopercular ampullary organ field; S, stage; st, supratemporal ampullary organ field; vi, ventral infraorbital ampullary organ field; vs, ventral supraorbital ampullary organ field. Scale bar: 200 μm.

'Hair cell' transcription factor genes expressed in developing ampullary organs include *Gfi1*, *Sox4* and *Sox3*

We previously showed that various transcription factor genes essential for hair cell development - *Six1*, *Eya1*, *Sox2*, *Atoh1*, *Pou4f3* (see Roccio et al., 2020; Iyer and Groves, 2021) - are expressed in developing paddlefish ampullary organs, as well as neuromasts (Modrell et al., 2011b; Modrell et al., 2011a; Butts et al., 2014; Modrell et al., 2017a). We confirm here that, in addition to *Sox2* (Figure 1E-H; Figure 2A,B), *Atoh1* and *Pou4f3* are also expressed in both types of lateral line organ in sterlet (Figure 2C-F). As noted earlier, *Sox2* was expressed more strongly in neuromasts than ampullary organs (Figure 1G,H; Figure 2A,B). However, *Atoh1* showed the converse pattern, with stronger expression in ampullary organs than in neuromasts (Figure 2C,D). These differential expression patterns were also seen at earlier stages (for *Sox2*, see Figure 1E-G; for *Atoh1*, see Supplementary Figure S2A-D).

A key 'hair cell' transcription factor gene whose expression we had not previously examined is the zinc-finger transcription factor gene *Gfi1* (see Roccio et al., 2020; Chen et al., 2021; Iyer and Groves, 2021; Iyer et al., 2022). *Gfi1* was 12.0-fold enriched in late-larval paddlefish operculum versus fin tissue (Modrell et al., 2017a). Sterlet *Gfi1* proved also to be expressed in developing ampullary organs, as well as neuromasts (Figure 2G,H).

In the mouse inner ear, the *SoxC* subfamily members *Sox4* and *Sox11* are co-expressed in proliferating hair cell progenitor cells and newly born hair cells, and in combination are essential for hair cell formation (Gnedeva and Hudspeth, 2015). Ectopic expression of either gene converts supporting cells to hair cells (Gnedeva and Hudspeth, 2015). Although neither *Sox4* nor *Sox11* was present in the paddlefish lateral line-enriched gene-set (Modrell et al., 2017a), we cloned sterlet *Sox4*, which proved to be expressed in both ampullary organs and neuromasts, though more strongly in ampullary organs (Figure 2I,J). This differential expression pattern was also seen at earlier stages (Supplementary Figure S2E-H).

It has been reported that proliferative stem cells in zebrafish neuromasts express the *SoxB1* subfamily member *Sox3*, as well as *Sox2*, and that *Sox3* is important for the formation of the correct number of neuromast hair cells (preprint: Undurraga et al., 2019). A recent single-cell RNA sequencing (scRNA-seq) study showed *Sox3* expression at homeostasis in multiple neuromast support cell types (Baek et al., 2022) including central cells, the immediate precursors of regenerating hair cells (Romero-Carvajal et al., 2015; Lush et al., 2019). We had previously used a candidate gene approach for lateral line placode markers to identify *Sox3* expression in paddlefish lateral line primordia, neuromasts and also ampullary organs (Modrell et al., 2011b). (*Sox3* was 5.2-fold enriched in late-larval paddlefish operculum versus fin tissue; Modrell et al., 2017a.) As expected, sterlet *Sox3* was also expressed in both types of

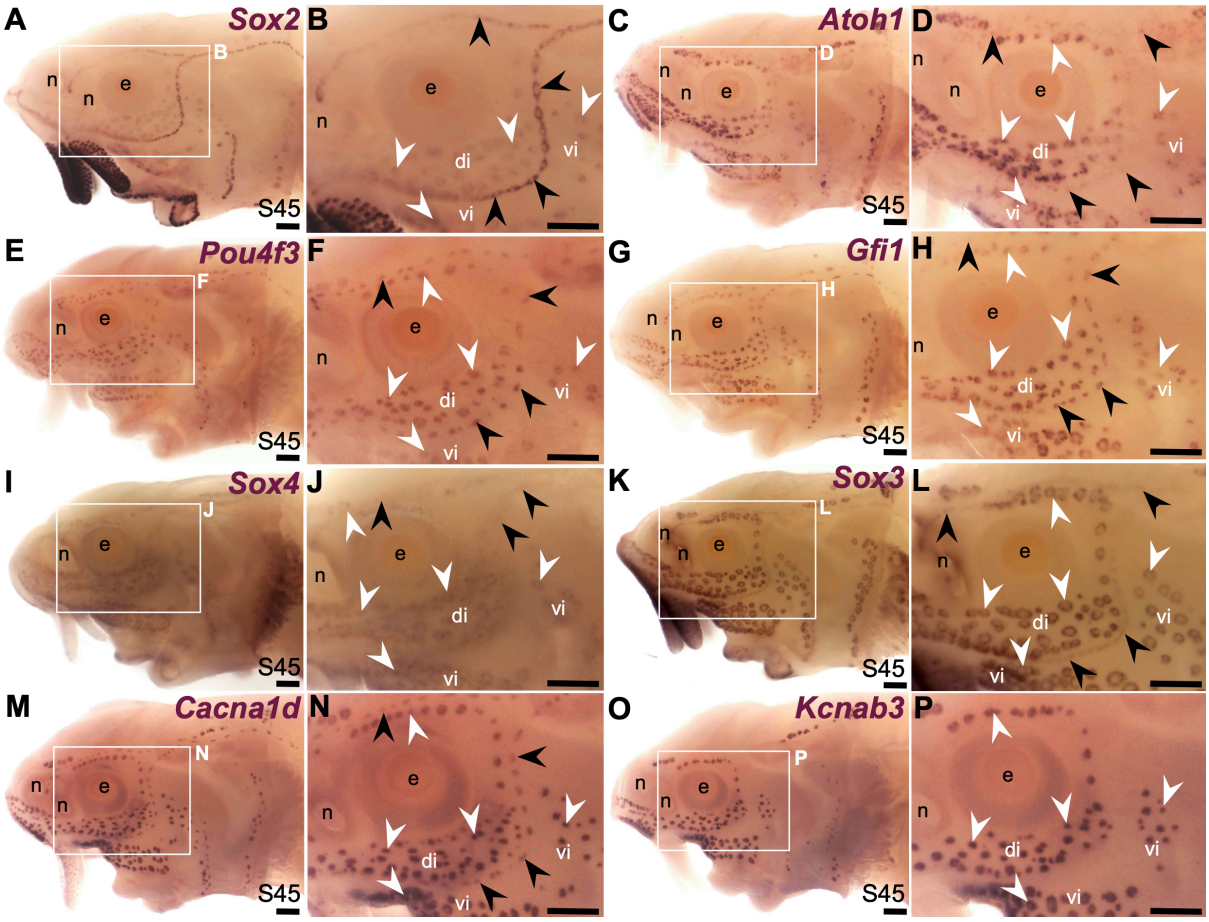

Figure 2. Transcription factor genes essential for hair cell development, including *Gfi1*, are expressed in ampullary organs as well as neuromasts. *In situ* hybridization in sterlet at stage 45 (the onset of independent feeding). Black arrowheads indicate examples of neuromasts; white arrowheads indicate examples of ampullary organs. (**A,B**) A paddlefish *Sox2* riboprobe reveals strong *Sox2* expression in neuromasts and weaker expression in ampullary organs (plus very strong expression in taste buds on the barbels and around the mouth). (**C,D**) *Atoh1* is expressed more strongly in ampullary organs than in neuromasts. (**E,F**) *Pou4f3* and (**G,H**) *Gfi1* are expressed in both neuromasts and ampullary organs. (**I,J**) *Sox4* is expressed in ampullary organs and very weakly in neuromasts. (**K,L**) *Sox3* expression is weaker in neuromasts than in ampullary organs (the opposite to *Sox2*; compare with A,B). (**M,N**) For comparison, the differentiated hair cell and electroreceptor marker *Cacna1d* is expressed in both neuromasts and ampullary organs (and also weakly in taste buds). (**O,P**) For comparison, the electroreceptor marker *Kcnab3* is expressed in ampullary organs only. Abbreviations: di, dorsal infraorbital ampullary organ field; e, eye; n, naris; S, stage; vi, ventral infraorbital ampullary organ field. Scale bar: 200 µm.

lateral line organ, though much more strongly in ampullary organs than in neuromasts (Figure 2K,L). Intriguingly, this was the opposite pattern to the other *SoxB1* family member, *Sox2* (Figure 2A,B). This differential expression pattern was also seen at earlier stages (Supplementary Figure S2I-L). For comparison, Figure 2M and 2N show the hair cell and electroreceptor marker *Cacna1d*, and Figure 2O and 2P show electroreceptor-specific *Kcnab3* expression.

Thus, all the key 'hair cell' transcription factors are expressed in developing ampullary organs as well as neuromasts (although several show differing levels of expression between

262 the different organ types). These results provide further support for the hypothesis that
263 electroreceptors evolved as transcriptionally related sister cell types to lateral line hair cells
264 (Baker and Modrell, 2018).
265
266 **Additional transcription factor genes expressed in developing ampullary organs and**
267 **neuromasts**
268 We cloned and analysed the expression of paddlefish and/or sterlet homologues of a further
269 33 transcription factor genes present in the late-larval paddlefish lateral line organ-enriched
270 dataset (Modrell et al., 2017a). (The paddlefish lateral line-enriched dataset also includes
271 fifteen other loci assigned to specific transcription factor/co-factor genes, for which cloning
272 and/or ISH failed in sterlet, or expression was inconsistent: *Akna*, *Barx1, Egr2, Fev*, *Fhl2*, *Fhl5*,
273 *Litaf*, *Meis3*, *Nkx3-1*, *Not2*, *Osr1*, *Pou3f1*, *Spdef, Tbx22* and *Vgll3*.) Nine of the transcription
274 factor genes examined were expressed in developing ampullary organs as well as
275 neuromasts, like *Gfi1* (see previous section). One was the zinc-finger transcription factor gene
276 *Insm2* (19.9-fold lateral line-enriched in late-larval paddlefish; Modrell et al., 2017a), which
277 was expressed in both ampullary organs and neuromasts in paddlefish and sterlet (Figure 3A-
278 D). However, *Insm2* expression was much stronger in ampullary organs than in neuromasts;
279 indeed in sterlet, *Insm2* expression in neuromasts was often undetectable except in some
280 parts of the neuromast lines (Figure 3C,D). The PRD class homeobox transcription factor gene
281 *Otx1* (18.7-fold lateral line-enriched; Modrell et al., 2017a) similarly showed much stronger
282 expression in ampullary organs than in neuromasts in both paddlefish and sterlet (Figure 3E-
283 H). Also expressed in both ampullary organs and neuromasts were two other homeobox
284 transcription factor genes, encoding TALE class Irx1 (Figure 3I,J; originally unassigned locus
285 111072; 8.3-fold lateral line-enriched, Modrell et al., 2017a) and LIM class Lhx6 (Figure 3K,L;
286 originally unassigned locus 12855; 3.5-fold lateral line-enriched, Modrell et al., 2017a). (The
287 *Lhx6-like* riboprobe recognises sequence from the 3' untranslated region of *Lhx6-like* mRNA,
288 as annotated in the sterlet reference genome; Du et al., 2020.)
289 The Notch target and effector gene *Hey2* (2.9-fold lateral line-enriched, Modrell et al.,
290 2017b) was also expressed by both ampullary organs and neuromasts (Figure 3M,N). Three
291 originally unassigned loci in the paddlefish lateral line organ-enriched dataset (Modrell et al.,
292 2017a), all of whose closest UniProt matches had Pfam Hairy Orange and helix-loop-helix
293 DNA-binding domains (locus 52662, 2.7-fold lateral line-enriched; locus 27975, 2.9-fold lateral
294 line-enriched; locus 26264, 2.3-fold lateral line-enriched), proved to represent the related
295 Notch target and effector gene *Hes5*. We had previously published the expression of *Hes5* in
296 both ampullary organs and neuromasts in a study on the role of Notch signalling in ampullary
297 organ versus neuromast development in paddlefish (Modrell et al., 2017b).

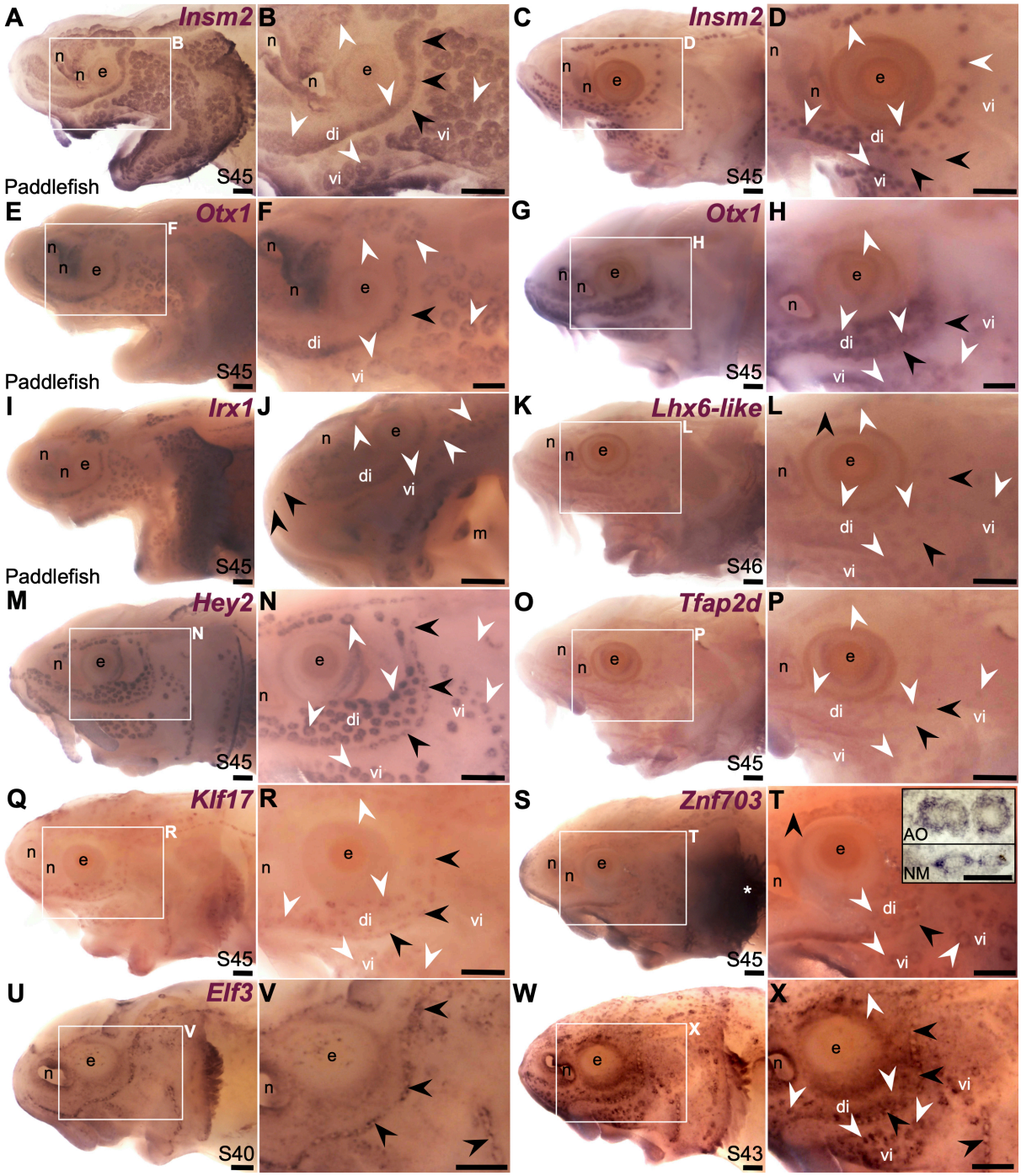

Figure 3. Other transcription factor genes expressed in ampullary organs and neuromasts. *In situ* hybridization in paddlefish or sterlet, showing genes expressed in both ampullary organs (white arrowheads indicate examples) and neuromasts (black arrowheads indicate examples). Higher power views in each case are of the same embryo shown in the preceding panel. (**A-D**) *Insm2* at stage 45 in paddlefish (A,B) and sterlet (C,D). Neuromast expression is only detectable in some parts of the neuromast lines and is noticeably weaker than in ampullary organs. (**E-H**) *Otx1* at stage 45 in paddlefish (E,F) and sterlet (G,H). Neuromast expression is considerably weaker than ampullary organ expression (almost undetectable in paddlefish). (**I,J**) *Irx1* at stage 45 in paddlefish. Neuromast expression is weak and can be seen most clearly on the tip of the rostrum (black arrowheads in J). (**K,L**) Sterlet *Lhx6-like* at stage 46. (**M,N**) Sterlet *Hey2* at stage 45. (**O,P**) Sterlet *Tfap2* at stage 45. (**Q,R**) Sterlet *Klf17* at stage 45. (**S,T**) Sterlet *Znf703* at stage 45. Expression in lateral line organs was often hard to detect in wholemount but expression in both neuromasts (NM) and ampullary organs (AO) was clear in skinmount (examples shown in inset in T). Strong expression is seen in gill filaments (white asterisk). (**U-X**) Sterlet *Elf3*. At stage 40 (U,V), *Elf3* is expressed in a 'ring' pattern in neuromasts, and in scattered

313 cells in the skin. By stage 43 (W,X), *Elf3* expression is also seen in ampullary organs and more broadly
314 throughout the skin. Abbreviations: AO, ampullary organ; di, dorsal infraorbital ampullary organ field; e,
315 eye; m, mouth; n, naris; NM, neuromast; S, stage; vi, ventral infraorbital ampullary organ field. Scale
316 bars: 200 μm except for inset in T: 50 μm.
317

318 Expression in developing ampullary organs and neuromasts was also seen for *Tfap2d*
319 (Figure 3O,P; 6.0-fold lateral line-enriched, Modrell et al., 2017a). This gene encodes
320 transcription factor AP-2 delta, which is a direct activator of *Pou4f3* in retinal ganglion cell
321 progenitors (Hesse et al., 2011; Li et al., 2016). The Krüppel-like transcription factor gene
322 *Klf17* (2.1-fold lateral line-enriched, originally annotated as *Klf4*; Modrell et al., 2017a) was
323 also expressed in both types of lateral line organ (Figure 3Q,R), as was the zinc finger
324 transcription factor gene *Znf703* (2.3-fold lateral line-enriched, Modrell et al., 2017a), although
325 neuromast expression was often at the limits of detection in wholemount (Figure 3S,T).
326 However, *Znf703* expression in neuromasts as well as ampullary organs was clear in
327 skinmount (Figure 3T, inset). The E74-like Ets domain transcription factor gene *Elf3* (2.1-fold
328 lateral line-enriched, Modrell et al., 2017a) showed a 'ring-like' expression pattern in both
329 neuromasts and ampullary organs that was clearer prior to stage 45 as general expression
330 gradually developed throughout the skin (Figure 3U-X).
331

332 **Electrosensory-restricted lateral line expression: *Irx5*, *Satb2*, *Insm1*, *Sp5*, *Mafa* and**
333 ***Rorc***

334 Our original analysis of candidates from the late-larval paddlefish lateral line organ-enriched
335 dataset identified the bHLH gene *Neurod4* as the first-reported transcription factor gene
336 restricted within the paddlefish lateral line to developing ampullary organs (Modrell et al.,
337 2017a). Here, we identified six more transcription factor genes whose lateral line expression
338 is restricted to ampullary organs in sterlet. Two encode homeodomain transcription factors:
339 the TALE class homeobox transcription factor gene *Irx5* (1.9-fold lateral line-enriched in
340 paddlefish, Modrell et al., 2017a; Figure 4A-D) and the CUT class (SATB subclass) homeobox
341 transcription factor gene *Satb2* (4.8-fold lateral line-enriched in paddlefish, Modrell et al.,
342 2017a), although its expression was weak (Figure 4E,F).

343 Two zinc-finger transcription factor genes similarly showed expression in sterlet
344 ampullary organs, but not neuromasts: *Insm1* (3.1-fold lateral line-enriched, Modrell et al.,
345 2017a; Figure 4G,H) and *Sp5* (2.6-fold lateral line-enriched, Modrell et al., 2017a; Figure 4I,J).
346 *Sp5* was also expressed in the migrating posterior lateral line primordium on the trunk, but not
347 in trunk neuromasts (Figure 4K: compare with *Sox2* expression in the migrating primordium
348 and developing neuromasts at the same stage, Figure 4L). (*Insm1* was also expressed in cells
349 scattered throughout the skin; these are likely to be Merkel cells, which were shown to express
350 *Insm1* in differential RNA-seq data from mouse; Hoffman et al., 2018.)

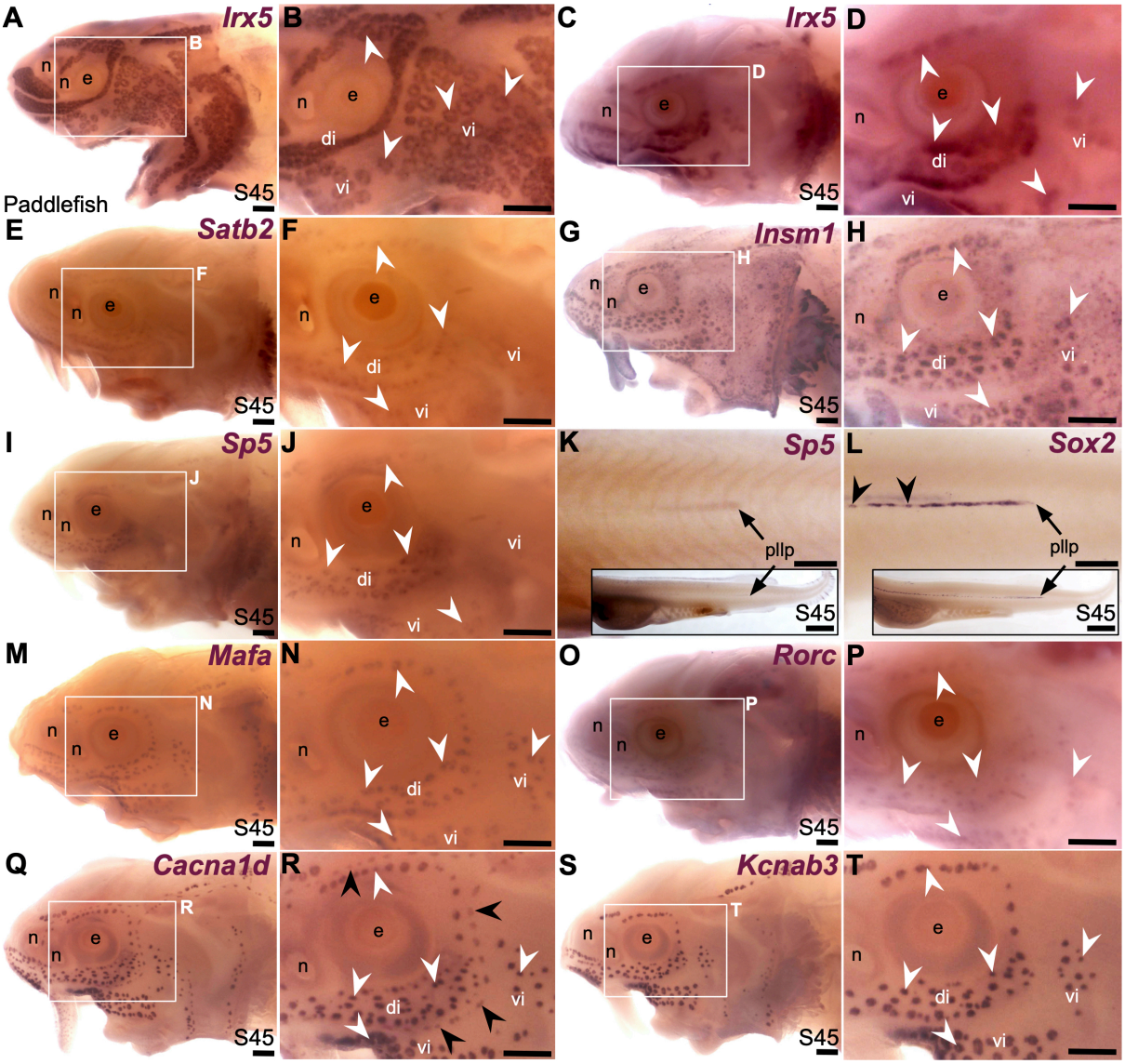

Figure 4. Transcription factor genes expressed in ampullary organs but not neuromasts. *In situ* hybridization at stage 45 in paddlefish or sterlet. White arrowheads indicate examples of ampullary organs; black arrowheads indicate examples of neuromasts. (**A-D**) *Irx5* in paddlefish (A,B) and sterlet (C,D; using the paddlefish riboprobe). (**E,F**) Sterlet *Satb2*. (**G,H**) Sterlet *Insm1* (also expressed in scattered cells throughout the skin, most likely Merkel cells). (**I-K**) Sterlet *Sp5*. Expression on the head is detected in ampullary organs but not neuromasts; on the trunk, weak expression is also visible in the migrating posterior lateral line primordium (arrow in K, different larva). The inset shows the position of the migrating primordium on the larval tail. (**L**) For comparison with panel K: *Sox2* expression (using a paddlefish *Sox2* riboprobe) is also seen in the migrating posterior lateral line primordium (arrow), as well as in developing neuromasts (black arrowheads). The inset shows the position of the migrating primordium on the larval tail. (**M,N**) Sterlet *Mafa*. (**O,P**) Sterlet *Rorc*. (**Q,R**) Sterlet *Cacna1d* for comparison, showing differentiated hair cells in neuromasts and electroreceptors in ampullary organs. (**S,T**) Sterlet *Kcnab3* for comparison, showing differentiated electroreceptors only. Abbreviations: di, dorsal infraorbital ampullary organ field; e, eye; n, naris; pllp, posterior lateral line primordium; S, stage; vi, ventral infraorbital ampullary organ field. Scale bars: 200 µm except for insets in K,L: 1000 µm.

Two other transcription factor genes proved to be expressed in ampullary organs but not neuromasts: the bZIP transcription factor gene *Mafa* (2.6-fold lateral line-enriched, Modrell et al., 2017a; Figure 4M,N) and a retinoic acid receptor (RAR)-related orphan nuclear receptor

371 gene, *Rorc* (14.3-fold lateral line-enriched, Modrell et al., 2017a; Figure 4O,P). For comparison
372 with the ampullary organ-restricted expression of the above-listed transcription factor genes,
373 Figure 4Q,R show *Cacna1d* expression in hair cells and electroreceptors, while Figure 4S,T
374 show electroreceptor-specific *Kcnab3* expression.
375
376 ***Sox8* is restricted to the mechanosensory lateral line in bony but not cartilaginous**
377 **fishes**
378 The paddlefish lateral line organ-enriched gene-set included a single *SoxE*-class high-mobility
379 group (HMG)-box transcription factor gene, *Sox10* (3.9-fold lateral line-enriched, Modrell et
380 al., 2017a). Comparison with the hair cell and electroreceptor marker *Cacna1d* (Figure 5A,B)
381 and the supporting cell marker *Sox2* (Figure 5C,D) shows that paddlefish *Sox10* was not
382 expressed within neuromasts or ampullary organs, but instead along nerves (Figure 5E,F).
383 *Sox10* expression would be expected in nerve-associated Schwann cells, as these neural
384 crest-derived glial cells express *Sox10* throughout their development and into the adult (see
385 e.g., Jessen and Mirsky, 2019).
386 Another *SoxE*-class HMG-box transcription factor gene, *Sox8*, was previously reported
387 to be expressed in developing ampullary organs in a shark, *Scyliorhinus canicula* (Freitas et
388 al., 2006). Given this, we also cloned *Sox8* and the remaining *SoxE* class gene, *Sox9*, to test
389 their expression in paddlefish. *Sox9* was expressed at late-larval stages in both neuromasts
390 and ampullary organs with a 'ring-like' distribution (Figure 5G,H). This is also consistent with
391 Sox9 expression in the developing mouse inner ear, where initial broad expression becomes
392 restricted to supporting cells, co-expressed with Sox2 (Mak et al., 2009; Jan et al., 2021).
393 Paddlefish *Sox8* expression, in contrast to *Sox9*, was restricted to neuromasts at late-
394 larval stages (Figure 5I,J), also in a ring pattern suggestive of supporting cells rather than
395 centrally clustered hair cells (compare neuromast expression of *Sox8* in Figure 5J with
396 *Cacna1d* in hair cells in Figure 5B and *Sox2* expression in supporting cells in Figure 5D). *Sox8*
397 was also expressed in neuromasts on the trunk (Figure 5K), and at earlier stages, in the central
398 region of sensory ridges where neuromasts form (Figure 5L).
399 The mechanosensory lateral line-restricted expression of paddlefish *Sox8* contrasts
400 with the reported expression of *Sox8* in shark ampullary organs (Freitas et al., 2006). To test
401 this further, we cloned all three *SoxE* genes from the lesser-spotted catshark (*Scyliorhinus*
402 *canicula*). We confirmed that *Sox8* is expressed in shark ampullary organs, as previously
403 reported (Freitas et al., 2006), as well as in neuromasts (Figure 5M,N), unlike the neuromast-
404 specific *Sox8* expression seen in the late-larval paddlefish (Figure 5K,L). *Sox9* was not
405 expressed in shark lateral line organs at all (Figure 5O,P), in striking contrast to paddlefish
406 *Sox9* expression in both neuromasts and ampullary organs (Figure 5G,H). The only conserved

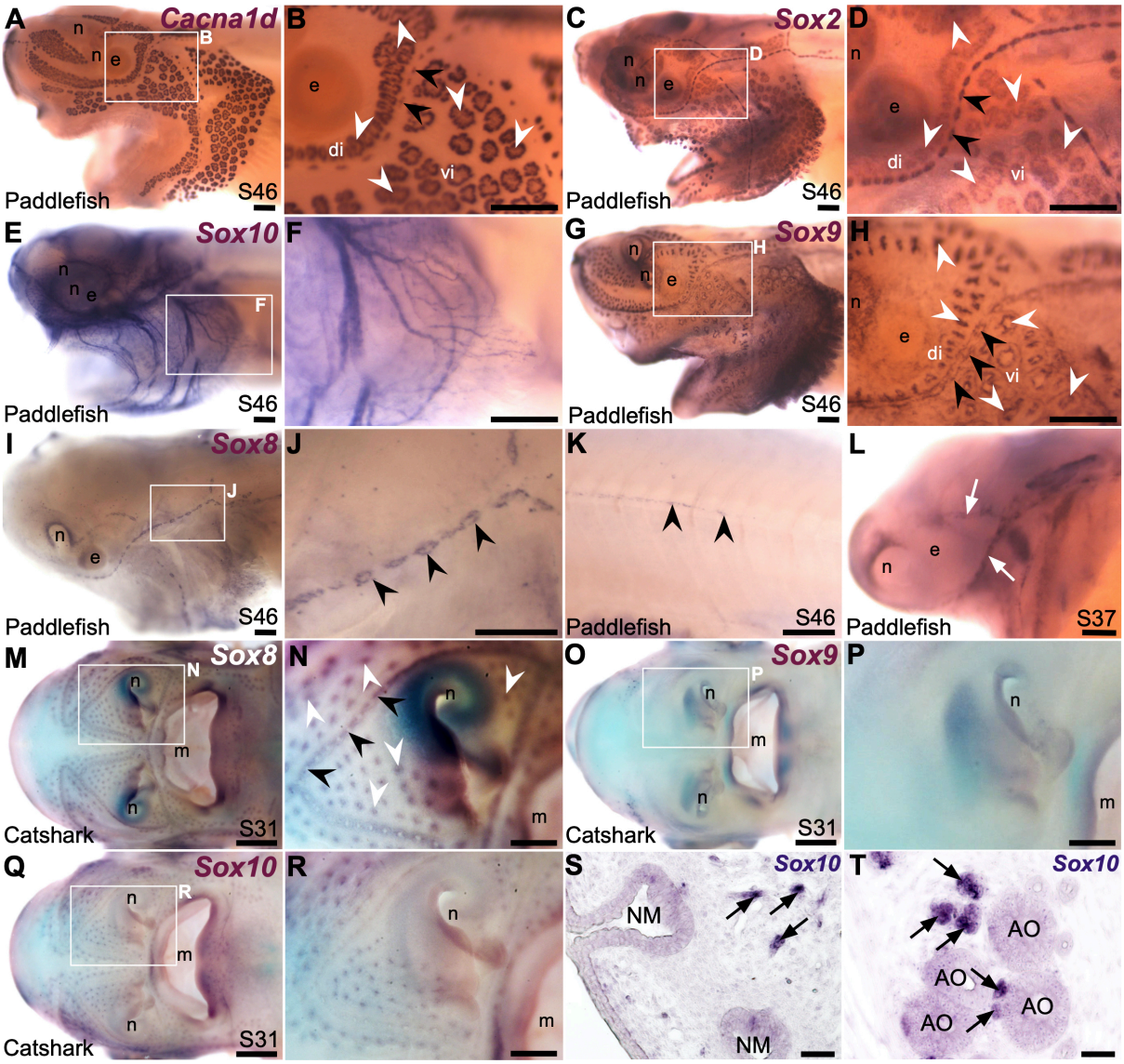

Figure 5. Lateral line expression of *SoxE* genes differs between chondrostean ray-finned bony fishes and cartilaginous fishes. *In situ* hybridization in late-larval paddlefish or catshark (*S. canicula*). White arrowheads indicate examples of ampullary organs; black arrowheads indicate examples of neuromasts. (**A,B**) For comparison, paddlefish *Cacna1d* expression at stage 46 reveals differentiated hair cells in neuromasts and electroreceptors in ampullary organs. (**C,D**) For comparison, paddlefish *Sox2* expression at stage 46 identifies support cells in neuromasts and ampullary organs. (**E,F**) Paddlefish *Sox10* expression at stage 46 is associated with cranial nerves, not in lateral line organs (compare with *Cacna1d* expression in panel A). (**G,H**) Paddlefish *Sox9* at stage 46 is expressed in a 'ring'-like pattern in neuromasts and ampullary organs (compare with panels A-D, especially in the ventral infraorbital ampullary organ field). (**I-K**) Paddlefish *Sox8* expression at stage 46 is seen in a ring pattern in neuromasts only (compare panel J with panels B,D), including in neuromasts developing on the trunk (K). (**L**) At stage 37, paddlefish *Sox8* is expressed in sensory ridges (white arrows). (**M,N**) Catshark *Sox8* at stage 31 is expressed in both neuromasts and ampullary organs. (**O,P**) Catshark *Sox9* expression at stage 31 is not seen in lateral line organs (compare with *Sox8* in panels O,P). (**Q-T**) Catshark *Sox10* expression at stage 31 seems to be in or near individual lateral line organs in whole-mount (Q,R). However, *in situ* hybridization on sections shows that *Sox10* is strongly expressed in cells (arrows) adjacent to neuromasts (S) and ampullary organs (T) that are likely associated with nerves. Above-background *Sox10* expression is not seen in the lateral line organs themselves. Abbreviations: di, dorsal infraorbital ampullary organ field; e, eye; m, mouth; n, naris; S, stage; vi, ventral infraorbital ampullary organ field. Scale bars: A-L,N,P,R, 200 µm; M,O,Q, 500 µm; S,T, 10 µm.

429 *SoxE* lateral line expression pattern between catshark and paddlefish was that of *Sox10*,
430 which ISH on sections confirmed to be restricted to axon-associated Schwann cells (Figure
431 5Q-T). Overall, these data reveal lineage-specific differences in *SoxE* transcription factor gene
432 expression within late-larval lateral line organs in a ray-finned chondrostean fish versus a
433 cartilaginous fish.
434
435 **_Foxg1_ is restricted to the mechanosensory lateral line**
436 The winged-helix transcription factor gene *Foxg1* was 11.4-fold enriched in late-larval (stage
437 46) paddlefish operculum vs. fin (Modrell et al., 2017a). *Foxg1* proved to be restricted to the
438 mechanosensory lateral line in ray-finned chondrostean fishes. For comparison, Figure 6A-D
439 show Sox2 protein expression in supporting cells in neuromasts and (more weakly) in
440 ampullary organs in late-larval paddlefish (Figure 6A,B) and sterlet (Figure 6C,D). Sox2
441 immunostaining also labels taste buds, and individual cells scattered throughout the skin (most
442 likely Merkel cells, which express Sox2 in zebrafish, as well as mouse; Brown et al., 2023;
443 Bardot et al., 2013; Lesko et al., 2013; Perdigoto et al., 2014). Paddlefish *Foxg1* expression
444 in the lateral line system at stage 45 (Figure 6E,F) was restricted to neuromast lines, but
445 excluded from the central domain of individual neuromasts where hair cells are found
446 (compare Figure 6F with Sox2 in Figure 6B). (*Foxg1* expression was also seen in the olfactory
447 system, as expected; e.g., Kawauchi et al., 2009.) Paddlefish *Foxg1* was expressed in the
448 migrating posterior lateral line primordium on the trunk, and in trunk neuromasts deposited by
449 the primordium (Figure 6G; compare with Sox2 immunostaining at the same stage, Figure
450 6H). Sterlet *Foxg1* was expressed in the same pattern at stage 45 as in paddlefish (Figure 6I-
451 K; Figure 6L shows Sox2 immunostaining in the sterlet posterior lateral line primordium and
452 trunk neuromasts for comparison with sterlet *Foxg1* expression in Figure 6K). Analysis at
453 earlier stages in sterlet showed that *Foxg1* expression was restricted to the central zone of
454 sensory ridges where neuromasts form (Figure 6M-R). Thus, *Foxg1* expression in the
455 developing lateral line system is restricted to the mechanosensory division, although it seems
456 to be excluded from differentiated hair cells.
457
458 **Mechanosensory-restricted lateral line expression of _Hmx2_, _Isl1_ and _Rorb_**
459 The NKL class homeobox transcription factor gene *Hmx2* (also known as *Nkx5-2*), which was
460 5.8-fold lateral line-enriched in late-larval paddlefish (Modrell et al., 2017a), also proved to be
461 restricted to the mechanosensory lateral line. For comparison, Figure 7A,B show Sox2
462 immunostaining at stage 45. At this stage, *Hmx2* was expressed in a ring-like pattern at the
463 outer edge of developing neuromasts (Figure 7C,D; compare with Sox2 in Figure 7A,B).

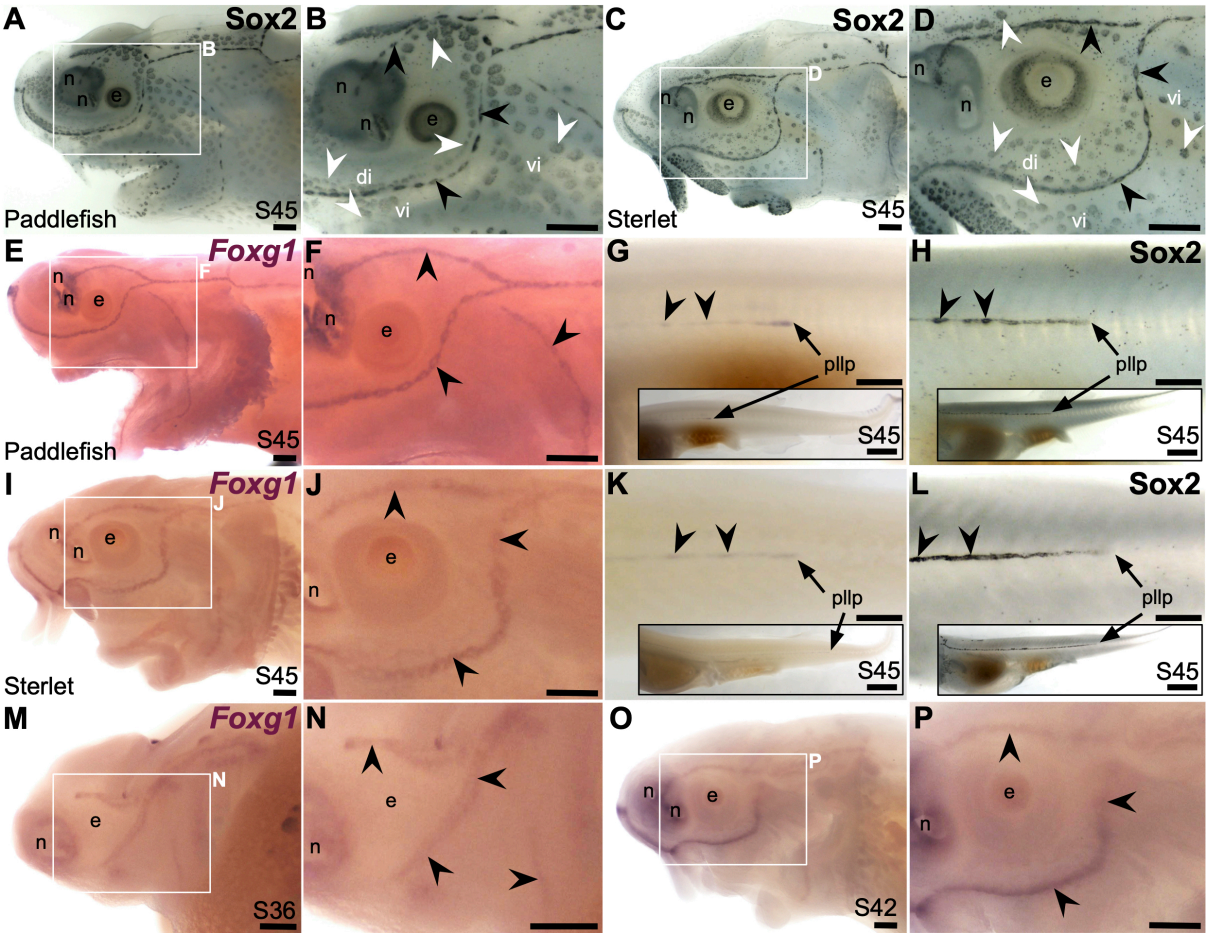

Figure 6. *Foxg1* is mechanosensory-restricted within the developing lateral line. Black arrowheads indicate examples of neuromasts; white arrowheads indicate examples of ampullary organs. (**A-D**) For comparison, Sox2 immunostaining at stage 45 in paddlefish (A,B) and sterlet (C,D) shows support cells in neuromasts (stronger staining) and ampullary organs (weaker staining). (Strong Sox2 expression is also seen in taste buds on the barbels and around the mouth, and in scattered cells in the skin, most likely Merkel cells.) (**E-G**) *In situ* hybridization for *Foxg1* at stage 45 in paddlefish, showing a ring-like expression pattern in the neuromast lines (compare panel F with paddlefish Sox2 in B), as well as expression in the migrating posterior lateral line primordium (arrow in G, different larva) and developing trunk neuromasts (black arrowheads). Expression is also seen in the nares. The inset in G shows the position of the migrating primordium on the larval tail. (**H**) For comparison with G, Sox2 immunostaining on the trunk at stage 45 in paddlefish shows the migrating posterior lateral line primordium (arrow) and developing neuromasts. The inset shows the position of the migrating primordium on the larval tail. (**I-K**) *In situ* hybridization for *Foxg1* at stage 45 in sterlet similarly shows a ring pattern in neuromasts (compare panel J with sterlet Sox2 in D), as well as expression in the migrating posterior lateral line primordium (arrow in K, different larva) and developing trunk neuromasts (black arrowheads). Expression is also seen in the nares. The inset in K shows the position of the migrating primordium on the larval tail. (**L**) For comparison with K, Sox2 immunostaining on the trunk at stage 45 in sterlet shows weak expression in the migrating posterior lateral line primordium (arrow) and developing neuromasts. The inset shows the position of the migrating primordium on the larval tail. (**M-P**) *In situ* hybridization for sterlet *Foxg1* at stage 36 (M,N) and stage 42 (O,P) shows ring-like expression already in developing neuromasts in sensory ridges, and no expression in developing ampullary organ fields (compare with sterlet *Eya4* expression at stages 35 and 41 in Figure 1A,C). Abbreviations: di, dorsal infraorbital ampullary organ field; e, eye; n, naris; pllp, posterior lateral line primordium; S, stage; vi, ventral infraorbital ampullary organ field. Scale bars 200 µm except for insets in G,H,K,L: 1000 µm.

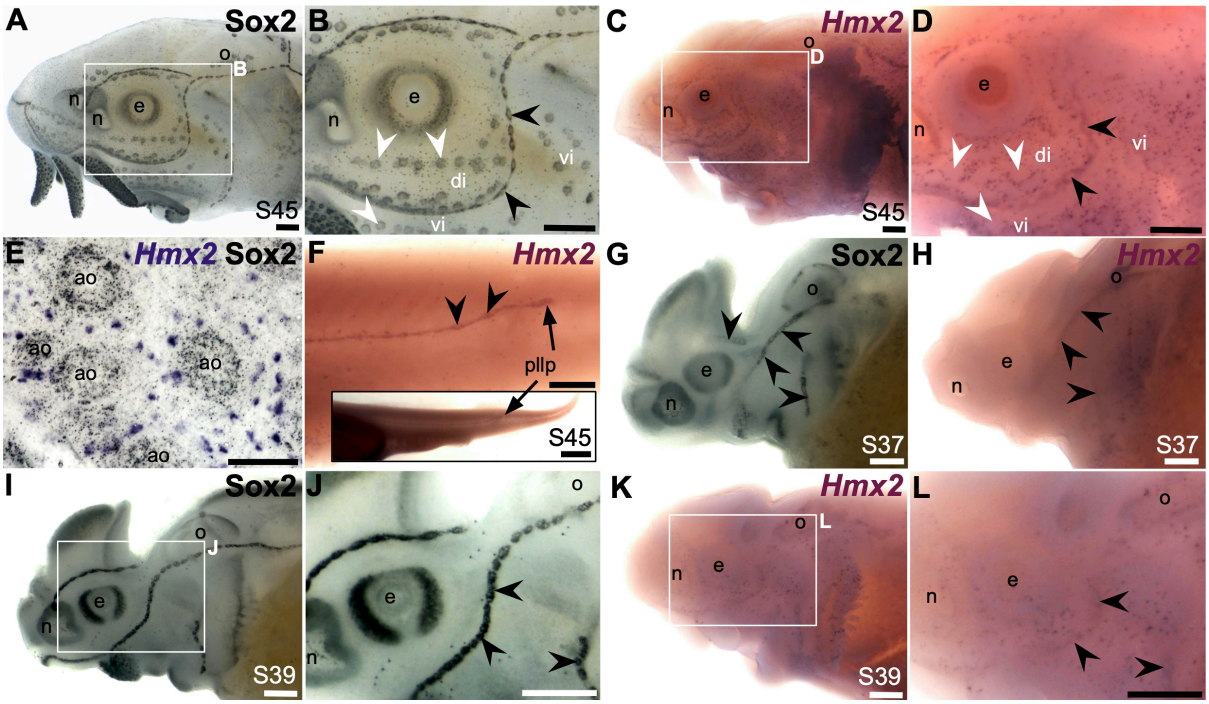

Figure 7. *Hmx2* is mechanosensory-restricted within the developing lateral line system. Black arrowheads indicate examples of neuromasts; white arrowheads indicate examples of ampullary organs. (**A,B**) For comparison, Sox2 immunostaining in sterlet is shown at stage 45. Sox2 labels developing neuromasts (stronger staining) and scattered cells in the skin, most likely Merkel cells, as well as taste buds on the barbels and around the mouth. Expression is also seen in ampullary organs (weaker than in neuromasts). A patch of Sox2 expression at the spiracular opening (first gill cleft) may represent the spiracular organ. (**C-F**) *In situ* hybridization for sterlet *Hmx2* at stage 45 in wholemount (C,D), *Hmx2* is weakly expressed in a ring-like pattern in the neuromast lines, as well as in scattered cells in the skin, but appears to be absent from ampullary organs (compare D with Sox2 expression in B). A skinmount (E) with several ampullary organs from a stage 45 embryo revealed by post-ISH immunostaining for Sox2 (black metallographic deposits) confirms that ampullary organs do not express *Hmx2* (purple). (The scattered *Hmx2*-positive skin cells may co-express Sox2, suggesting they are likely to be Merkel cells.) *Hmx2* is also expressed in the trunk neuromast line (F), including the migrating posterior lateral line primordium (black arrow in J). The inset shows the position of the migrating primordium on the larval tail. (**G**) For comparison with H, Sox2 immunostaining at stage 37 labels developing neuromasts. Expression is also seen in the nasal capsule and otic vesicle, as well as eye. (**H**) *Hmx2* expression at stage 37 is detected in neuromast lines, as well as in the otic vesicle. (**I,J**) For comparison with K and L, Sox2 immunostaining at stage 39 labels developing neuromasts and scattered cells in the skin, most likely Merkel cells, as well as taste buds on the barbels. Expression is also seen in the nasal capsule and the eye. (**K,L**) *Hmx2* expression at stage 39 is detected in neuromast lines and scattered cells in the skin. Abbreviations: ao, ampullary organ; di, dorsal infraorbital ampullary organ field; e, eye; n, naris; o, otic vesicle; pllp, posterior lateral line primordium; S, stage; vi, ventral infraorbital ampullary organ field. Scale bars: 200 µm except for panel E: 50 µm and inset in F, 1000 µm.

However, no expression was seen in ampullary organs (Figure 7C,D), confirmed in skinmounts after post-ISH Sox2 immunostaining to identify ampullary organs (Figure 7E). As an aside, *Hmx2* expression was also seen in scattered skin cells (Figure 7C-E). *Hmx2* was not among the genes reported in a differential RNA sequencing study of adult mouse Merkel cells (Hoffman et al., 2018). However, examination of sterlet skinmounts after post-ISH Sox2 immunostaining suggested the *Hmx2*-expressing skin cells may co-express Sox2 (Figure 7E),

524 which would support their being Merkel cells. Alternatively, other scRNA-seq studies in mouse
525 and human have shown that *Hmx2* is expressed by tuft (brush) cells in gut and airway epithelia
526 (Haber et al., 2017; Deprez et al., 2020), so it is possible the *Hmx2*-expressing skin cells in
527 paddlefish are chemosensory epithelial cells, like tuft cells (Kotas et al., 2023).
528 *Hmx2* was also expressed in the migrating posterior lateral line primordium at stage
529 45 (Figure 7F), like *Foxg1* (Figure 6K) and Sox2 (Figure 6L). Analysis at earlier stages, with
530 Sox2 immunostaining for comparison (Figure 7G-L), showed that *Hmx2* was weakly
531 expressed in neuromast lines (and in the otic vesicle) at stage 37 (Figure 7H; compare with
532 Sox2 in Figure 7G) and at stage 39 (Figure 7K,L; compare with Sox2 in Figure 7I,J).
533 The LIM class homeobox transcription factor Isl1 was recently reported to promote a
534 more complete conversion by Atoh1 of mouse cochlear supporting cells to hair cells than does
535 Atoh1 alone (Yamashita et al., 2018). The only LIM homeobox genes in the paddlefish lateral
536 line organ-enriched dataset (Modrell et al., 2017a) are *Lhx3*, which we previously reported to
537 be expressed in ampullary organs as well as neuromasts (Modrell et al., 2017a); *Lhx6-like*
538 (originally unassigned locus 12855), with the same expression pattern (Figure 3K), and *Lhx8*,
539 which proved to be expressed in gill filaments, not lateral line organs (Supplementary Figure
540 S3J). Nevertheless, given the demonstrated role for Isl1 in promoting cochlear hair cell
541 formation (Yamashita et al., 2018), we cloned sterlet *Isl1*. For comparison, Figure 8A,B show
542 Sox2 immunostaining at stage 45, and Figure 8C,D show *Cacna1d*-expressing hair cells and
543 electroreceptors at stage 45. At this stage, *Isl1* expression was weak, but restricted within the
544 lateral line system to neuromasts (Figure 8E,F). Examination at earlier stages revealed no
545 detectable expression at stage 36 (Figure 8G,H) and neuromast-restricted expression at
546 stages 39 and 40, when *Isl1* seemed to be more strongly expressed than at stage 45 (Figure
547 8I-L).
548 Finally, we identified the RAR-related orphan nuclear receptor beta gene, *Rorb* (6.2-
549 fold lateral line-enriched; Modrell et al., 2017a), as being also restricted to neuromasts, with
550 no detectable expression in ampullary organs (Figure 8M-P). The onset of *Rorb* expression in
551 neuromasts was later even than *Isl1*, starting only at stage 41 (Figure 8M,N). It was intriguing
552 to see the mutually exclusive expression of *Rorb* in neuromasts (Figure 8O,P) and *Rorc* in
553 ampullary organs (Figure 4O,P).
554 Taken together, we have identified *Sox8*, *Foxg1*, *Hmx2*, *Isl1* and *Rorb* as the first-
555 reported transcription factor genes restricted to the mechanosensory division of the lateral line
556 system in ray-finned fishes. *Sox8* and *Foxg1* are expressed in the central zone of sensory
557 ridges where neuromasts form and maintained in neuromasts, though apparently excluded
558 from differentiated hair cells. *Hmx2* is expressed in sensory ridges and retained in neuromasts,
559 whereas *Isl1* and *Rorb* are restricted to neuromasts as early as they can be detected.
560 The remaining transcription factor genes from the paddlefish lateral line organ-

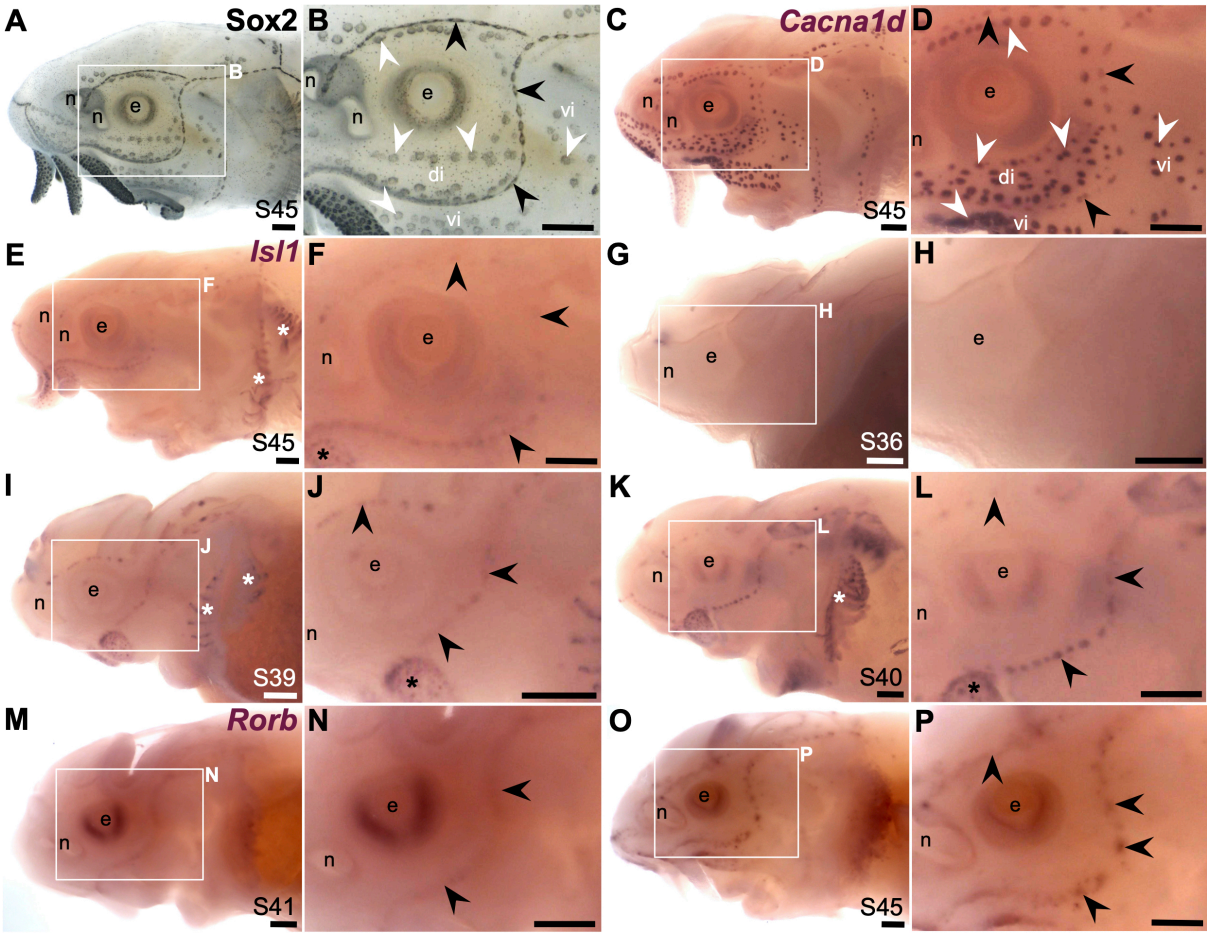

Figure 8. *Isl1* and *Rorb* are mechanosensory-restricted within the developing lateral line system. Black arrowheads indicate examples of neuromasts; white arrowheads indicate examples of ampullary organs. (**A,B**) For comparison, Sox2 immunostaining in sterlet is shown at stage 45. Sox2 labels developing neuromasts (stronger staining) and scattered cells in the skin, most likely Merkel cells, as well as taste buds on the barbels and around the mouth. Expression is also seen in ampullary organs (weaker than in neuromasts). A patch of Sox2 expression at the spiracular opening (first gill cleft) may represent the spiracular organ. (**C,D**) For comparison, *in situ* hybridization for sterlet *Cacna1d* at stage 45 shows expression in hair cells in neuromasts and electroreceptors in ampullary organs (and weak expression in taste buds on the barbels). (**E,F**) *In situ* hybridization for sterlet *Isl1* at stage 45 shows weak spots of expression in neuromasts but not ampullary organs (compare with *Cacna1d* in C,D). Stronger expression is seen in taste buds on the barbels (black asterisk) and in gill filaments (white asterisk). (**G-L)** *In situ* hybridization for sterlet *Isl1* at earlier stages shows no expression at stage 36 (G,H), and expression in neuromasts (but not ampullary organs) at stage 39 (I,J), and stage 40 (K,L). From stage 39, *Isl1* expression is also seen in taste buds on the barbels (asterisk in J) and in gill filaments. (**M-P**) *In situ* hybridization for sterlet *Rorb* at stage 41 (M,N), and stage 45 (O,P) shows neuromast-specific expression within the lateral line. Abbreviations: di, dorsal infraorbital ampullary organ field; e, eye; n, naris; pllp, posterior lateral line primordium; S, stage; vi, ventral infraorbital ampullary organ field. Scale bars: 200 µm.

enriched gene-set that we examined proved not to be expressed in lateral line organs, but instead, e.g., in ectoderm around ampullary organs (Supplementary Figure S3A-D: *Ehf*, *Foxi2* and *Nkx2-3*), or at the edge of the operculum, in taste buds and/or in developing gill filaments (Supplementary Figure S3E-P: *Foxe1*, *Foxl2*, *Gcm2*, *Hoxa2*, *Lhx8*, *Pou3f4*, *Sim2*, *Tbx1*, *Tlx1*, *Tlx2* and *Rax2*).

586

587 **Discussion**

588

589 In this study, we used our paddlefish lateral line organ-enriched gene-set (generated from
590 differential bulk RNA-seq at late larval stages; Modrell et al., 2017a), together with a candidate
591 gene approach, to identify 23 novel transcription factor genes expressed in developing lateral
592 line organs in sterlet and/or paddlefish. These data, together with our previous work in
593 paddlefish (Modrell et al., 2011b; Modrell et al., 2011a; Modrell et al., 2017b; Modrell et al.,
594 2017a), suggest extensive conservation of molecular mechanisms involved in electrosensory
595 and mechanosensory lateral line organ development. However, they also reveal a set of
596 transcription factor genes with restricted expression that may be involved in the development
597 of mechanosensory versus electrosensory organs. Of the 40 transcription factor genes with
598 validated expression during lateral line organ development in paddlefish and/or sterlet, 28
599 (70%) were expressed in both ampullary organs and neuromasts (Table 1). These include the
600 key 'hair cell' transcription factor genes *Six1*, *Eya1*, *Sox2*, *Atoh1*, *Pou4f3* and *Gfi1* (see Roccio
601 et al., 2020; Chen et al., 2021; Iyer and Groves, 2021; Iyer et al., 2022). We also identified
602 seven electrosensory-restricted and five mechanosensory-restricted transcription factor
603 genes (Table 1), as discussed further below.

604 While this work was ongoing, a differential RNA-seq study of regenerating ampullary
605 organs and neuromasts in the Siberian sturgeon (*Acipenser baerii*) was published (Wang et
606 al., 2020). This study compared dissected tissue samples containing stage 45 ampullary
607 organs or neuromasts relative to general epidermis, which identified 2074 lateral line organ-
608 enriched genes, of which 1418 were shared by ampullary organs and neuromasts; 539 were
609 ampullary organ-enriched, and 117 were neuromast-enriched (Wang et al., 2020). The
610 'common' stage 45 lateral line-organ dataset from the Siberian sturgeon (Wang et al., 2020)
611 included many of the candidate genes encoding transcription factors and differentiation
612 markers whose expression we have validated in both ampullary organs and neuromasts at
613 stage 45-46 in paddlefish and/or sterlet, e.g. *Six1*, *Eya1*, *Atoh1*, *Pou4f3*, *Gfi1*, *Otof,* and
614 *Cacna1d* (Modrell et al., 2011b; Modrell et al., 2011a; Modrell et al., 2017a; this study). The
615 ampullary organ-enriched dataset from the Siberian sturgeon (Wang et al., 2020) included
616 *Sp5*, which we identified here in sterlet as ampullary organ-restricted, but also *Hmx2* and *Rorb*,
617 which we identified here as neuromast-restricted. Conversely, the neuromast-enriched
618 dataset (Wang et al., 2020) included *Insm1*, which we found in sterlet to be ampullary organ-
619 restricted. Furthermore, the 'common' dataset (Wang et al., 2020) included genes whose
620 expression in sterlet and paddlefish was either ampullary organ-specific (e.g., the voltage-
621 gated K^+ channel genes *Kcna5* and *Kcnab3*, as well as *Neurod4*; this study; Modrell et al.,
622 2017a), or mechanosensory-specific (e.g., *Foxg1* and *Isl1*; this study).

Overall, we think that the stage 45 Siberian sturgeon tissue dissections (Wang et al., 2020) were unable to separate ampullary organs and neuromasts completely. Like our own stage 46 paddlefish lateral line organ-enriched dataset (Modrell et al., 2017a), the stage 45 Siberian sturgeon datasets are not exhaustive (Wang et al., 2020): some of the genes whose expression we have validated in stage 45-46 sterlet and/or paddlefish lateral line organs were missing (e.g., *Satb2*, *Sox2* and *Sox8*; this study; Modrell et al., 2017a). Nevertheless, this differential RNA-seq study in late-larval Siberian sturgeon embryos (Wang et al., 2020) provides an invaluable, independent resource from which to identify additional candidate genes for future validation and functional investigation *in vivo*.

Conserved molecular mechanisms are likely involved in the formation of electroreceptors and hair cells

In this study, we identified twelve novel transcription factor genes expressed in both types of lateral line organ in chondrostean ray-finned fishes, consistent with conservation of molecular mechanisms. In particular, we highlight *Gfi1* (see Roccio et al., 2020; Chen et al., 2021; Iyer and Groves, 2021; Iyer et al., 2022) as being another key 'hair cell' transcription factor gene expressed in developing ampullary organs as well as neuromasts, together with *Atoh1*, *Pou4f3*, and *Six1* (Modrell et al., 2011a; Modrell et al., 2017a). *Gfi1*-deficient hair cells fail to mature and also upregulate neuronal differentiation genes such as *Neurod1* and *Pouf41*, suggesting that a key function of Gfi1 in hair cells is to repress neuronal genes that are initially also expressed in hair cell progenitors (Matern et al., 2020). Gfi1 also acts indirectly to increase Atoh1 transcriptional activity, by forming part of a transcriptional complex with Atoh1 and E proteins, in which neither Atoh1 nor Gfi1 binds the other directly and Gfi1 does not bind DNA (Jen et al., 2022). Given shared expression in ampullary organs as well as neuromasts, it seems likely that Gfi1 plays these roles in developing electroreceptors, as well as hair cells. Intriguingly, however, *Insm2* was recently reported as a direct target of both Atoh1 and Gfi1 in mouse cochlear hair cells, and one of only a handful of genes (including *Atoh1* itself) to be repressed by Gfi1 during hair-cell maturation (Jen et al., 2022). Repression of *Insm2* by Gfi1 in mature hair cells, but not electroreceptors, could explain the much weaker expression of *Insm2* that we saw in neuromasts versus ampullary organs at stage 45 (the onset of independent feeding). This suggests the existence of both shared and divergent functions of the same transcription factor within hair cells versus electroreceptors.

Six novel ampullary organ-restricted transcription factor genes

We have identified six novel transcription factor genes expressed in developing ampullary organs but not neuromasts in chondrostean ray-finned fishes, in addition to previously published *Neurod4* (Modrell et al., 2017a). Two of these, *Irx5* and *Satb2*, encode

660 homeodomain transcription factors. In *C. elegans*, unique combinations of homeodomain
661 transcription factors define all 118 neuron classes (Reilly et al., 2020) (also see Vidal et al.,
662 2022). Hence, members of this class of transcription factors are potentially good candidates
663 to be involved in controlling divergent fate specification and/or maintenance in closely related
664 cell types.

665 *Irx5* is required for the terminal differentiation of a subset of cone bipolar cells in the
666 mouse retina (Cheng et al., 2005). In mouse and chicken, *Irx5* is expressed within the otic
667 vesicle epithelium, including some prospective sensory patches (Bosse et al., 2000; Cardeña-
668 Núñez et al., 2016). However, by stage 34 in chicken (embryonic day 8), when hair cells are
669 fully differentiated, *Irx5* is not expressed in any sensory patch, unlike some other *Irx* family
670 members (Cardeña-Núñez et al., 2016). In mouse, chicken and zebrafish, *Irx5* (together with
671 other *Irx* family members) is expressed in otic placode-derived neurons (Bosse et al., 2000;
672 Houweling et al., 2001; Cardeña-Núñez et al., 2016; Lecaudey et al., 2005). In zebrafish, the
673 only reported expression of *Irx5a* in the lateral line system is in the secondary posterior lateral
674 line primordium (prim II) (Lecaudey et al., 2005). This migrates later than the primary posterior
675 lateral line primordium and contributes post-embryonically to lateral and dorsal branches of
676 the trunk lateral line (Sapède et al., 2002). However, the function of *Irx5* in the primordium is
677 not known (Lecaudey et al., 2005) and the lack of reported expression in neuromasts is
678 consistent with its restriction to ampullary organs in paddlefish and sterlet.

679 Ampullary organ-restricted *Satb2* encodes a homeodomain transcription factor and
680 chromatin-remodeller that is important for craniofacial development, including osteoblast
681 differentiation (reviewed by Huang et al., 2022). Its expression has not been reported in the
682 inner ear or lateral line system. The *Satb2* gene is directly bound by Smad1/5 and upregulated
683 following over-expression of *Bmp4* in cranial neural crest cells, suggesting that *Satb2* is a
684 direct target of the Bmp signalling pathway (Bonilla-Claudio et al., 2012). This raises the
685 possibility that Bmp signalling may be important for ampullary organ development. Indeed,
686 *Bmp4*, *Bmp5*, *Brinp3* (encoding BMP/retinoic acid-inducible neural-specific protein 3) and
687 *Bambi* (encoding a Bmp/activin inhibitor) are present in the 'common' lateral line organ-
688 enriched gene-set from stage 45 Siberian sturgeon (Wang et al., 2020). *Brinp3* is also in the
689 ampullary organ-enriched gene-set (Wang et al., 2020). Our stage 46 paddlefish lateral line
690 organ-enriched gene-set also includes *Bmp5*, together with genes encoding the dual Bmp/Wnt
691 inhibitors Sostdc1 and Apcdd1 (Modrell et al., 2017a). Thus, the Bmp pathway is a promising
692 target for studies of ampullary organ development.

693 The other electrosensory-restricted transcription factor genes were *Insm1*, *Mafa*, *Rorc*
694 and *Sp5*. In the inner ear, transient expression of Insm1 in developing outer hair cells prevents
695 them from transdifferentiating into inner hair cells, by repressing a set of genes usually

696 enriched in early inner hair cells (Wiwatpanit et al., 2018). It is possible, therefore, that Insm1
697 also acts in developing ampullary organs to repress hair cell-specific genes.
698 MafA synergises with Neurod1 (and Pdx1) to activate the *insulin* promoter in pancreatic
699 beta-cells (reviewed in Liang et al., 2022). Given the ampullary organ-restricted expression of
700 *Neurod4* in the paddlefish lateral line system (Modrell et al., 2017a), this raises the possibility
701 that MafA could similarly synergise with Neurod4 to activate ampullary organ-specific target
702 genes.
703 *Rorc* encodes two isoforms of a ligand-dependent transcription factor, RAR-related
704 orphan nuclear receptor gamma (RORγ and RORγt), primarily studied for its roles in regulating
705 Th17 cell differentiation and thus autoimmune and inflammatory diseases (see Fauber and
706 Magnuson, 2014; Meijer et al., 2020; Ladurner et al., 2021). Endogenous ligands for RORγ
707 have not been confirmed, but it responds to sterols including the cholesterol precursor,
708 desmosterol (see Hu et al., 2015; Meijer et al., 2020). Retinoic acid has also been reported to
709 inhibit RORγ activity (Stehlin-Gaon et al., 2003). In the axolotl, ampullary organs were missing
710 and far fewer cranial neuromasts formed after retinoic acid treatment for one hour at late
711 gastrula/early neurula stages (Gibbs and Northcutt, 2004b). However, this most likely reflects
712 an effect on the lateral line placodes themselves, rather than organ formation directly (Gibbs
713 and Northcutt, 2004b). In any case, the mutually exclusive expression of ampullary organ-
714 restricted *Rorc* and neuromast-restricted *Rorb* is particularly intriguing (also see next section).
715 Finally, *Sp5* encodes a Wnt/β-catenin effector (Kennedy et al., 2016), suggesting that
716 this signalling pathway might be important for ampullary organ development. Indeed, one of
717 the other ampullary organ-restricted genes, *Irx5*, is directly upregulated by Wnt/β-catenin
718 signalling in somatic cells of the gonad (Koth et al., 2020).
719 Overall, the ampullary organ-restricted expression of these six transcription factor
720 genes provides a starting point for identifying molecular mechanisms that may be important
721 for the formation of electrosensory lateral line organs.
722
723 **Five novel mechanosensory lateral line-restricted transcription factor genes**
724 We identified five mechanosensory lateral line-restricted transcription factor genes: the first-
725 such genes reported in electroreceptive vertebrates. Of these, *Hmx2*, *Isl1* and *Rorb* are
726 expressed in zebrafish lateral line placodes and/or neuromasts (Feng and Xu, 2010; Dufourcq
727 et al., 2006; Bertrand et al., 2007). *Hmx2* and *Isl1* both encode homeodomain transcription
728 factors. In zebrafish, *Hmx2* is expressed throughout lateral line placode development, together
729 with the related gene *Hmx3* (Feng and Xu, 2010). Morpholino knockdown experiments
730 suggested a redundant requirement for *Hmx2* and *Hmx3* for cell proliferation in the migrating
731 posterior lateral line primordium, and for normal neuromast formation (Feng and Xu, 2010).
732 Double mutant analysis of *Hmx2* and *Hmx3a* suggested that the loss of neuromasts arises

733 from stalling of the migrating primordium adjacent to the first few somites, hence failure to
734 deposit neuromasts (England et al., 2020). Recent scRNA-seq data from zebrafish also show
735 that *Hmx2* is expressed specifically in anterior-posterior (A/P) support cells in neuromasts
736 (Baek et al., 2022).

737 We cloned *Isl1* because it promotes a more complete conversion by Atoh1 of mouse
738 cochlear supporting cells to hair cells than does Atoh1 alone (Yamashita et al., 2018). In
739 zebrafish neuromasts, *Isl1* is expressed in multiple support cell types including central support
740 cells (Lush et al., 2019; Baek et al., 2022), which divide symmetrically to form new hair cells
741 after hair cells are ablated (Romero-Carvajal et al., 2015; Lush et al., 2019). In neural crest-
742 derived sensory ganglia, Isl1 is expressed in all neurons and is necessary for nociceptor
743 lineage-specific gene expression, for repressing earlier-acting neurogenic transcription factors
744 - including direct repression of *Neurod4*, which is ampullary organ-specific in the paddlefish
745 lateral line (Modrell et al., 2017a) - and for repressing lineage-inappropriate genes (Sun et al.,
746 2008; Dykes et al., 2011). In the pancreas, Isl1 is a direct transcriptional repressor of *Mafa*
747 (Du et al., 2009), which we identified here as ampullary organ-restricted (see previous
748 section). We hypothesize that, in electroreceptive species, Isl1 may promote a hair cell fate
749 within neuromasts at least in part by repressing an electroreceptor fate, including by
750 repressing *Neurod4* and *Mafa*.

751 *Rorb*, encoding RAR-related orphan nuclear receptor beta (RORβ), is expressed by
752 supporting cells in adult and embryonic neuromasts in zebrafish (Dufourcq et al., 2006;
753 Bertrand et al., 2007). Retinoic acid is a confirmed inhibitory ligand for RORβ (Stehlin-Gaon
754 et al., 2003). The reciprocal expression of *Rorb* in neuromasts and *Rorc* in ampullary organs
755 (see previous section) suggests that these ligand-dependent transcription factors play specific
756 roles in the development of mechanosensory versus electrosensory organs.

757 In contrast to *Hmx2*, *Isl1* and *Rorb*, mechanosensory lateral line-restricted *Foxg1* and
758 *Sox8* are not expressed in the developing lateral line system of zebrafish or *Xenopus* (e.g.,
759 Dirksen and Jamrich, 1995; Papalopulu and Kintner, 1996; Toresson et al., 1998; Eagleson
760 and Dempewolf, 2002; Duggan et al., 2008; Zhao et al., 2009; O'Donnell et al., 2006; Martik
761 et al., 2019). As zebrafish and *Xenopus* only have a mechanosensory lateral line system
762 (Baker et al., 2013; Baker, 2019), this suggests *Foxg1* and *Sox8* may play specific roles in the
763 developing mechanosensory lateral line system of electroreceptive bony vertebrates, rather
764 than in lateral line primordium or neuromast development *per se*. (In cartilaginous fishes, i.e.,
765 sharks, *Sox8* is expressed in ampullary organs as well as neuromasts; this study and (Freitas
766 et al., 2006)

767 In paddlefish and sterlet, *Foxg1* was expressed in the central zones of lateral line
768 sensory ridges where neuromasts form, though excluded from the central domains of
769 neuromasts where hair cells differentiate. In the mouse olfactory epithelium, Foxg1 maintains

770 a proliferative Sox2$^+$ progenitor state (Kawauchi et al., 2009). Similarly, in the inner ear, Foxg1
771 is expressed by Sox2$^+$ hair cell progenitors and supporting cells in sensory epithelia (Kiernan
772 et al., 2005; Dabdoub et al., 2008; Tasdemir-Yilmaz et al., 2021), although it is also expressed
773 by a subset of hair cells (Pauley et al., 2006). *Foxg1* mouse mutants have reduced inner ear
774 sensory epithelia and a shortened cochlea with numerous additional rows of disorganized hair
775 cells (Pauley et al., 2006; Hwang et al., 2009). Conditional knockout of *Foxg1* in supporting
776 cells in the neonatal mouse inner ear resulted in increased numbers of hair cells, potentially
777 by transdifferentiation of supporting cells (Zhang et al., 2019; Zhang et al., 2020). Overall,
778 *Foxg1* is an exciting candidate for further investigation at the functional level.
779 Recent work on otic placode development in chicken embryos (Buzzi et al., 2022)
780 suggests that another of the chondrostean lateral line mechanosensory-restricted transcription
781 factors we identified, *Sox8*, could play an even earlier role than *Foxg1*. (*Sox8* was expressed
782 in ampullary organs as well as neuromasts in cartilaginous fishes, however, suggesting
783 lineage-specific divergence of expression between cartilaginous and bony vertebrates.) Sox8
784 in chicken lies upstream of all other transcription factor genes in the otic gene regulatory
785 network, including *Foxg1* (Buzzi et al., 2022). Ectopic expression of *Sox8* in cranial ectoderm
786 drives the formation of ectopic otic vesicles and neurons (Buzzi et al., 2022). In paddlefish,
787 *Sox8* displays a similar expression pattern to *Foxg1* in elongating lateral line primordia and
788 neuromasts. As mentioned, *Sox8* expression has not been reported in the developing lateral
789 line system in either *Xenopus* or zebrafish (O'Donnell et al., 2006; Martik et al., 2019). Given
790 the 'master regulator' role of *Sox8* in otic placode development (Buzzi et al., 2022), it is
791 possible that *Sox8* lies upstream of *Foxg1* in lateral line primordium development specifically
792 in electroreceptive vertebrates (although it may play a separate, later role in ampullary organ
793 development in cartilaginous fishes).
794
795 **Conclusion**
796 The data presented here, taken together with our previous results in paddlefish (Modrell et al.,
797 2011b; Modrell et al., 2011a; Modrell et al., 2017b; Modrell et al., 2017a), show that most
798 transcription factor genes expressed in developing lateral line organs in chondrostean ray-
799 finned fishes, including many that are required for hair cell development, are expressed in both
800 ampullary organs and neuromasts. This supports the hypothesis that the molecular
801 mechanisms underlying electrosensory and mechanosensory lateral line organ development
802 are highly conserved, and that electroreceptors likely evolved as transcriptionally related sister
803 cell types to lateral line hair cells (Modrell et al., 2017a; Baker and Modrell, 2018). Moreover,
804 in addition to ampullary organ-restricted *Neurod4* (Modrell et al., 2017a), we have identified a
805 further eleven transcription factors (six that are electrosensory-restricted; five that are
806 mechanosensory-restricted) that could be involved in the formation of electrosensory versus

807 mechanosensory organs. These are good candidates for functional experiments using
808 CRISPR/Cas9-mediated mutagenesis in sterlet (e.g., Chen et al., 2018; Baloch et al., 2019;
809 Stundl et al., 2022), the next step to further our understanding of the development of these
810 sensory (sister) cell types.
811
812 **Materials and Methods**
813
814 **Embryo collection, staging and fixation**
815 Fertilized sterlet (*Acipenser ruthenus*) eggs were obtained from adults bred at the Research
816 Institute of Fish Culture and Hydrobiology (RIFCH), Faculty of Fisheries and Protection of
817 Waters, University of South Bohemia in České Budějovice, Vodňany, Czech Republic. Sterlet
818 animal husbandry, *in vitro* fertilization and the rearing of embryos and yolk-sac larvae are
819 described in detail in Stundl et al. (2022). Sterlet embryos were staged according to Dettlaff et
820 al. (1993). Animal care was approved by the Ministry of Agriculture of the Czech Republic
821 (MSMT-12550/2016-3), followed the principles of the European Union Harmonized Animal
822 Welfare Act of the Czech Republic, and Principles of Laboratory Animal Care and National
823 Laws 246/1992 "Animal Welfare", and was conducted in accordance with the Animal Research
824 Committee of RIFCH.
825 Mississippi paddlefish (*Polyodon spathula*) embryos were purchased from Osage
826 Catfisheries Inc. (Osage Beach, MO, USA) and reared at approximately 22°C in tanks with
827 filtered and recirculating water (pH 7.2 ± 0.7, salinity of 1.0 ± 0.2 ppt). Paddlefish embryos
828 were staged according to Bemis and Grande (1992). Lesser-spotted catshark (*Scyliorhinus*
829 *canicula*) egg cases were reared in a flow-through seawater system at the Station Biologique
830 de Roscoff, France. Catshark embryos were staged according to Ballard et al. (1993).
831 Upon reaching desired developmental stages, embryos/larvae of all three species
832 were euthanized via overdose of MS-222 (Sigma-Aldrich). Paddlefish and sterlet
833 embryos/yolk-sac larvae were fixed in modified Carnoy's fixative (6 volumes 100% ethanol: 3
834 volumes 37% formaldehyde: 1 volume glacial acetic acid) for 3 hours at room temperature or
835 for 12-24 hours at 4°C, then dehydrated stepwise into ethanol and stored at -20°C. Catshark
836 embryos were fixed overnight at 4°C in 4% paraformaldehyde in phosphate-buffered saline
837 (PBS), washed three times in PBS, dehydrated stepwise into methanol and stored at -20°C.
838
839 **Generation of *de novo* transcriptome assemblies from late-larval sterlet heads**
840 Sterlet yolk-sac larvae intended for RNA isolation were preserved in RNAlater (Invitrogen,
841 Thermo Fisher Scientific) and stored at -80°C until processed. Prior to RNA isolation, RNAlater
842 was removed, and heads were manually dissected from sterlet yolk-sac larvae: two at stage
843 40, two at stage 42, three at stage 45. RNA was then extracted using TRIzol reagent

844 (Invitrogen, Thermo Fisher Scientific) according to the manufacturer's instructions. RNA
845 concentration was assessed using a Nanodrop N1000 spectrophotometer and integrity using
846 an Agilent 2100 Bioanalyzer (Cambridge Genomic Services, Department of Pathology,
847 University of Cambridge, UK). Samples with an RNA integrity number (RIN) greater than 9
848 were submitted for next-generation sequencing at The Centre for Applied Genomics, The
849 Hospital for Sick Children, Toronto, Canada. Libraries were prepared using the NEBNExt Ultra
850 Directional RNA library prep kit and sequenced on an Illumina HiSeq 2500, using Illumina v3
851 chemistry, following the multiplex paired-end protocol (2 x 125 bases).
852 Reads were subjected to various quality controls, including high-quality read filtering
853 based on the score value given in fastq files (FastQC version 0.10.1;
854 http://www.bioinformatics.babraham.ac.uk/projects/fastqc/), removal of reads
855 containing primer/adaptor sequences and read-length trimming using Trimmomatic-0.30
856 (Bolger et al., 2014). *De novo* assembly was performed using Velvet version 1.2.10 (Zerbino
857 and Birney, 2008) and Oases version 0.2.08 (Schulz et al., 2012). Velvet was run using
858 different k-mer lengths, k31, k43, k47, k53 and k63 along with other default parameters. Oases
859 was run using the same k-mer range. Results from these assemblies were merged, using
860 Velvet and Oases k-mer of k43. All assemblies were performed on a server with 64 cores and
861 512 GB of RAM. A second *de novo* assembly was carried out using Trinity version 2.6.6
862 (Grabherr et al., 2011) using default parameters. This Transcriptome Shotgun Assembly
863 project has been deposited at DDBJ/EMBL/GenBank under the accessions GKLU00000000
864 (Velvet-Oases assembly) and GKEF00000000 (Trinity assembly). The versions described in
865 this paper are the first versions, GKLU00000000 and GKEF01000000.
866
867 **Gene cloning and sequence verification**
868 Total RNA was isolated from embryos using Trizol (Invitrogen, Thermo Fisher Scientific),
869 following the manufacturer's protocol, and cDNA made using the Superscript III First Strand
870 Synthesis kit (Invitrogen, Thermo Fisher Scientific). To design gene-specific PCR primers or
871 synthetic gene fragments for paddlefish or sterlet, we used the previously published paddlefish
872 transcriptome assembly (NCBI Gene Expression Omnibus accession code GSE92470;
873 Modrell et al., 2017a) or the sterlet transcriptome assemblies reported here (deposited at
874 DDBJ/EMBL/GenBank under the accessions GKLU00000000 and GKEF01000000). To
875 design gene-specific PCR primers for lesser-spotted catshark, we used *S. canicula* RNAseq
876 data, publicly available via the Skatebase website (http://skatebase.org/skateblast-
877 skatebase%e2%80%8b/). Gene-specific primers (Supplementary file 1) were used to amplify
878 cDNA fragments under standard PCR conditions from cDNA and cloned into the pDrive
879 cloning vector (Qiagen) as previously described (Modrell et al., 2011a). Catshark cDNA
880 fragments were cloned into the pGEM-T Easy vector (Promega). Alternatively, synthetic gene

881 fragments based on paddlefish or sterlet transcriptome data, with added M13 forward and
882 reverse primer adaptors, were ordered from Twist Bioscience. GenBank accession numbers
883 for sterlet (*A. ruthenus*), paddlefish (*P. spathula*) and catshark (*S. canicula*) cDNA fragments
884 are given in Supplementary file 1.
885 Individual clones were verified by sequencing (Department of Biochemistry
886 Sequencing Facility, University of Cambridge, UK, or Genewiz, Azenta Life Sciences, UK).
887 Sequence identity was checked using the National Center for Biotechnology Information
888 (NCBI) Basic Local Alignment Search Tool (BLAST; https://blast.ncbi.nlm.nih.gov/Blast.cgi;
889 McGinnis and Madden, 2004). Where BLAST results were inconclusive in establishing
890 sequence identity, we performed phylogenetic analysis using PhyML 3.0 (http://www.atgc-
891 montpellier.fr/phyml/; Guindon et al., 2010), including related amino acid sequences available
892 from the UniProt database (https://www.uniprot.org/; UniProt, 2023). Sterlet sequences whose
893 identity was still inconclusive following phylogenetic analysis were checked by BLAST against
894 the sterlet reference genome (Du et al., 2020).
895
896 ***In situ* hybridization and immunohistochemistry**
897 Digoxigenin-labelled antisense riboprobes were synthesized from cloned cDNA fragments
898 (Supplementary file 1) using T7 or SP6 polymerases (Promega) and digoxigenin-labeled
899 dUTPs (Roche). Alternatively, synthetic gene fragments (Twist Bioscience) with added M13
900 forward and reverse primer adaptors were PCR-amplified under standard conditions using the
901 M13 forward primer, and the M13 reverse primer containing an overhang with the SP6
902 polymerase promoter. The PCR product was then used as a template for riboprobe synthesis
903 by *in vitro* transcription using SP6 polymerase and digoxigenin-labeled dUTPs (Roche). Each
904 riboprobe was tested a minimum of two times, using at least three embryos per stage.
905 Whole-mount in situ hybridization (ISH) was performed as previously described
906 (Modrell et al., 2011a). In some cases, sterlet and paddlefish yolk-sac larvae were processed
907 into pre-hybridization buffer as described (Modrell et al., 2011a), then stored at -20°C for up
908 to a month in this solution before continuing the protocol. For weaker riboprobes, overnight
909 incubations at 4°C in MABT (0.1 M maleic acid, 150 mM NaCl, 0.1% Tween-20, pH 7.5) and/or
910 NTMT (100 mM NaCl, 100 mM Tris, pH 9.5, 50 mM MgCl2, 0.1% Tween-20) were added prior
911 to the colour reaction, to increase the signal to background staining ratio.
912 Whole-mount immunostaining was performed as previously described (Metscher and
913 Müller, 2011). When using sterlet embryos or yolk-sac larvae that had not already been subject
914 to ISH, bleaching and proteinase K treatment were performed prior to immunostaining, as
915 described for ISH (Modrell et al., 2011a). A primary antibody against Sox2 (rabbit monoclonal,
916 ab92494; Abcam) was used at 1:200 and a horseradish peroxidase-conjugated goat anti-
917 rabbit antibody (Jackson ImmunoResearch) at 1:300. For the histochemical reaction, the

metallographic peroxidase substrate EnzMet kit (Nanoprobes) was used according to the manufacturer's instructions.

For skinmounts after whole-mount ISH and/or immunostaining, skin samples were dissected using forceps and microcapillary needles and mounted on Superfrost Plus slides (VWR) using Fluoroshield mounting medium with DAPI (Sigma-Aldrich).

For ISH on sections, embryos were embedded in paraffin wax and sectioned at 10 µm as previously described (O'Neill et al., 2007). ISH on sections was performed as previously described (O'Neill et al., 2007; Miller et al., 2017) except that slides were not treated with proteinase K prior to hybridization and BMP Purple (Roche) was used for the colour reaction.

Imaging and image processing

Whole-mount embryos and larvae were positioned in a slit in an agar-coated Petri dish with PBS and imaged using a Leica MZFLIII dissecting microscope equipped with a MicroPublisher 5.0 RTV camera (QImaging) or a MicroPublisher 6 color CCD camera (Teledyne Photometrics). Skinmounts and sections were imaged using a Zeiss AxioSkop 2 microscope equipped with a Retiga 2000R camera and RGB pancake (QImaging) or a MicroPublisher 6 color CCD camera (Teledyne Photometrics). Images were acquired using QCapture Pro 6.0 or 7.0 software (QImaging) or Ocular software (Teledyne Photometrics). For most whole-mount embryos and larvae, as well as skinmounts, a stack of images was taken by manually focusing through the sample, then focus stacking was performed using Helicon Focus software (Helicon Soft Limited). Images were processed in Adobe Photoshop (Adobe Systems Inc.).

Data availability statement

The Transcriptome Shotgun Assembly project has been deposited at DDBJ/EMBL/GenBank under the accessions GKLU00000000 and GKEF00000000. The versions described in this paper are the first versions, GKLU00000000 and GKEF00000000. The publication and associated supplementary figures include representative example images of embryos from each experiment. Additional raw data underlying this publication consist of further images of these and other embryos from each experiment. Public sharing of these images is not cost-efficient, but they are available from the corresponding author upon reasonable request.

Ethics statement

Sterlet animal work was reviewed and approved by The Animal Research Committee of Research Institute of Fish Culture and Hydrobiology, Faculty of Fisheries and Protection of Waters, University of South Bohemia in České Budějovice, Vodňany, Czech Republic and Ministry of Agriculture of the Czech Republic (MSMT-12550/2016-3).

Author contributions

CB conceived and designed the project with input from MSM, MM and AG, and wrote the manuscript together with MM. MM performed most of the experiments, prepared all the manuscript figures and made a significant contribution to the writing of the manuscript. MSM, AG, AC and IF performed some experiments. RL undertook the transcriptome assembly with support from GM. MP and DG were instrumental in enabling all work with sterlet embryos. All authors read and commented on the manuscript.

Funding

This work was supported by the Biotechnology and Biological Sciences Research Council (BB/F00818X/1 and BB/P001947/1 to CB), the Leverhulme Trust (RPG-383 to CB) and the Royal Society (Newton International Fellowship to AG). Additional support for MM was provided by the Cambridge Isaac Newton Trust (grant 20.07[c] to CB) and by the School of the Biological Sciences, University of Cambridge. AC was supported by a PhD research studentship from the Anatomical Society. The work of MP was supported by the Ministry of Education, Youth and Sports of the Czech Republic, projects CENAKVA (LM2018099), Biodiversity (CZ.02.1.01/0.0/0.0/16_025/0007370) and Czech Science Foundation (20-23836S). Collection of *S. canicula* embryos was funded by an Association of European Marine Biological Laboratories ASSEMBLE award to AG.

Rights Retention Statement

This work was funded by grants from the Biotechnology and Biological Sciences Research Council (BB/F00818X/1 and BB/P001947/1). For the purpose of open access, the author has applied a Creative Commons Attribution (CC BY) licence to any Author Accepted Manuscript version arising.

Acknowledgments

Thanks to Marek Rodina and Martin Kahanec for their help with sterlet spawns, and Michaela Vazačová for her help with embryo incubation and fixation. Thanks to Tatjana Piotrowski and her lab at the Stowers Institute for Medical Research (Kansas City, MO, USA) and Steve and Pete Kahrs and the Kahrs family (Osage Catfisheries, Inc.) for hosting MSM during paddlefish spawning seasons. Thanks to Christine Hirschberger and Rolf Ericsson for their help with some of the *in situ* hybridization rounds.

Conflict of Interest: The authors declare that the research was conducted in the absence of any commercial or financial relationships that could be construed as a potential conflict of interest.

References

Baek, S., Tran, N.T.T., Diaz, D.C., Tsai, Y.-Y., Acedo, J.N., Lush, M.E., Piotrowski, T., 2022. Single-cell transcriptome analysis reveals three sequential phases of gene expression during zebrafish sensory hair cell regeneration. Dev. Cell 57, 799-819.

Baker, C.V.H., 2019. The development and evolution of lateral line electroreceptors: insights from comparative molecular approaches., in: B.A. Carlson, J.A. Sisneros, A.N. Popper, R.R. Fay (Eds.), Electroreception: Fundamental Insights from Comparative Approaches. Springer, Cham, pp. 25-62.

Baker, C.V.H., Modrell, M.S., 2018. Insights into electroreceptor development and evolution from molecular comparisons with hair cells. Integr. Comp. Biol. 58, 329-340.

Baker, C.V.H., Modrell, M.S., Gillis, J.A., 2013. The evolution and development of vertebrate lateral line electroreceptors. J. Exp. Biol. 216, 2515-2522.

Ballard, W.W., Mellinger, J., Lechenault, H., 1993. A series of normal stages for development of *Scyliorhinus canicula*, the lesser spotted dogfish (*Chondrichthyes*: *Scylorhinidae*). J. Exp. Zool. 267, 318-336.

Baloch, A.R., Franěk, R., Tichopád, T., Fučíková, M., Rodina, M., Pšenička, M., 2019. *Dnd1* knockout in sturgeons by CRISPR/Cas9 generates germ cell free host for surrogate production. Animals (Basel) 9, 174.

Bardot, E.S., Valdes, V.J., Zhang, J., Perdigoto, C.N., Nicolis, S., Hearn, S.A., Silva, J.M., Ezhkova, E., 2013. Polycomb subunits Ezh1 and Ezh2 regulate the Merkel cell differentiation program in skin stem cells. EMBO J. 32, 1990-2000.

Bellono, N.W., Leitch, D.B., Julius, D., 2017. Molecular basis of ancestral vertebrate electroreception. Nature 543, 391-396.

Bellono, N.W., Leitch, D.B., Julius, D., 2018. Molecular tuning of electroreception in sharks and skates. Nature 558, 122-126.

Bemis, W.E., Grande, L., 1992. Early development of the actinopterygian head. I. External development and staging of the paddlefish *Polyodon spathula*. J. Morphol. 213, 47-83.

Bennett, M.V.L., Obara, S., 1986. Ionic mechanisms and pharmacology of electroreceptors, in: T.H. Bullock, W. Heiligenberg (Eds.), Electroreception. Wiley, New York, pp. 157-181.

Bertrand, S., Thisse, B., Tavares, R., Sachs, L., Chaumot, A., Bardet, P.L., Escrivà, H., Duffraisse, M., Marchand, O., Safi, R., Thisse, C., Laudet, V., 2007. Unexpected novel relational links uncovered by extensive developmental profiling of nuclear receptor expression. PLoS Genet. 3, e188.

1027 Bodznick, D., Montgomery, J.C., 2005. The physiology of low-frequency electrosensory
1028 systems, in: T.H. Bullock, C.D. Hopkins, A.N. Popper, R.R. Fay (Eds.), Electroreception.
1029 Springer, New York, pp. 132-153.
1030 Bolger, A.M., Lohse, M., Usadel, B., 2014. Trimmomatic: a flexible trimmer for Illumina
1031 sequence data. Bioinformatics 30, 2114-2120.
1032 Bonilla-Claudio, M., Wang, J., Bai, Y., Klysik, E., Selever, J., Martin, J.F., 2012. Bmp signaling
1033 regulates a dose-dependent transcriptional program to control facial skeletal
1034 development. Development 139, 709-719.
1035 Bosse, A., Stoykova, A., Nieselt-Struwe, K., Chowdhury, K., Copeland, N.G., Jenkins, N.A.,
1036 Gruss, P., 2000. Identification of a novel mouse Iroquois homeobox gene, *Irx5*, and
1037 chromosomal localisation of all members of the mouse Iroquois gene family. Dev. Dyn.
1038 218, 160-174.
1039 Brown, T.L., Horton, E.C., Craig, E.W., Goo, C.E.A., Black, E.C., Hewitt, M.N., Yee, N.G., Fan,
1040 E.T., Raible, D.W., Rasmussen, J.P., 2023. Dermal appendage-dependent patterning of
1041 zebrafish *atoh1a*+ Merkel cells. eLife 12, e85800.
1042 Butts, T., Modrell, M.S., Baker, C.V.H., Wingate, R.J.T., 2014. The evolution of the vertebrate
1043 cerebellum: absence of a proliferative external granule layer in a non-teleost ray-finned
1044 fish. Evol. Dev. 16, 92-100.
1045 Buzzi, A.L., Chen, J., Thiery, A., Delile, J., Streit, A., 2022. Sox8 remodels the cranial ectoderm
1046 to generate the ear. Proc. Natl. Acad. Sci. U.S.A. 119, e2118938119.
1047 Camacho, S., Ostos, M.D.V., Llorente, J.I., Sanz, A., García, M., Domezain, A., Carmona, R.,
1048 2007. Structural characteristics and development of ampullary organs in *Acipenser*
1049 *naccarii*. Anat. Rec. (Hoboken) 290, 1178-1189.
1050 Caprara, G.A., Peng, A.W., 2022. Mechanotransduction in mammalian sensory hair cells. Mol.
1051 Cell. Neurosci. 120, 103706.
1052 Cardeña-Núñez, S., Sánchez-Guardado, L.Ó., Corral-San-Miguel, R., Rodríguez-Gallardo, L.,
1053 Marín, F., Puelles, L., Aroca, P., Hidalgo-Sánchez, M., 2016. Expression patterns of Irx
1054 genes in the developing chick inner ear. Brain Struct. Funct. 222, 2071-2092.
1055 Chagnaud, B.P., Wilkens, L.A., Hofmann, M., 2021. The ampullary electrosensory system –a
1056 paddlefish case study, in: B. Fritzsch (Ed.), The Senses: A Comprehensive Reference.
1057 Elsevier, pp. 215-227.
1058 Chen, J., Wang, W., Tian, Z., Dong, Y., Dong, T., Zhu, H., Zhu, Z., Hu, H., Hu, W., 2018.
1059 Efficient gene transfer and gene editing in sterlet. Front. Genet. 9, 117.
1060 Chen, Y., Gu, Y., Li, Y., Li, G.L., Chai, R., Li, W., Li, H., 2021. Generation of mature and
1061 functional hair cells by co-expression of *Gfi1*, *Pou4f3*, and *Atoh1* in the postnatal mouse
1062 cochlea. Cell Rep. 35, 109016.

1063 Cheng, C.W., Chow, R.L., Lebel, M., Sakuma, R., Cheung, H.O.-L., Thanabalasingham, V.,
1064 Zhang, X., Bruneau, B.G., Birch, D.G., Hui, C.C., McInnes, R.R., Cheng, S.H., 2005. The
1065 *Iroquois* homeobox gene, *Irx5*, is required for retinal cone bipolar cell development. Dev.
1066 Biol. 287, 48-60.
1067 Crampton, W.G.R., 2019. Electroreception, electrogenesis and electric signal evolution. J.
1068 Fish Biol. 95, 92-134.
1069 Dabdoub, A., Puligilla, C., Jones, J.M., Fritzsch, B., Cheah, K.S., Pevny, L.H., Kelley, M.W.,
1070 2008. Sox2 signaling in prosensory domain specification and subsequent hair cell
1071 differentiation in the developing cochlea. Proc. Natl. Acad. Sci. U.S.A. 105, 18396-
1072 18401.
1073 Deprez, M., Zaragosi, L.E., Truchi, M., Becavin, C., Ruiz García, S., Arguel, M.J., Plaisant,
1074 M., Magnone, V., Lebrigand, K., Abelanet, S., Brau, F., Paquet, A., Pe'er, D., Marquette,
1075 C.H., Leroy, S., Barbry, P., 2020. A single-cell atlas of the human healthy airways. Am.
1076 J. Respir. Crit. Care Med. 202, 1636-1645.
1077 Dettlaff, T.A., Ginsburg, A.S., Schmalhausen, O.I., 1993. Sturgeon Fishes: Developmental
1078 Biology and Aquaculture. Springer-Verlag, Berlin.
1079 Dirksen, M.-L., Jamrich, M., 1995. Differential expression of *fork head* genes during early
1080 *Xenopus* and zebrafish development. Dev. Genet. 17, 107-116.
1081 Du, A., Hunter, C.S., Murray, J., Noble, D., Cai, C.-L., Evans, S.M., Stein, R., May, C.L., 2009.
1082 Islet-1 is required for the maturation, proliferation, and survival of the endocrine
1083 pancreas. Diabetes 58, 2059-2069.
1084 Du, K., Stöck, M., Kneitz, S., Klopp, C., Woltering, J.M., Adolfi, M.C., Feron, R., Prokopov, D.,
1085 Makunin, A., Kichigin, I., Schmidt, C., Fischer, P., Kuhl, H., Wuertz, S., Gessner, J.,
1086 Kloas, W., Cabau, C., Iampietro, C., Parrinello, H., Tomlinson, C., Journot, L.,
1087 Postlethwait, J.H., Braasch, I., Trifonov, V., Warren, W.C., Meyer, A., Guiguen, Y.,
1088 Schartl, M., 2020. The sterlet sturgeon genome sequence and the mechanisms of
1089 segmental rediploidization. Nat. Ecol. Evol. 4, 841-852.
1090 Dufourcq, P., Roussigné, M., Blader, P., Rosa, F., Peyrieras, N., Vriz, S., 2006. Mechano-
1091 sensory organ regeneration in adults: the zebrafish lateral line as a model. Mol. Cell.
1092 Neurosci. 33, 180-187.
1093 Duggan, C.D., Demaria, S., Baudhuin, A., Stafford, D., Ngai, J., 2008. Foxg1 is required for
1094 development of the vertebrate olfactory system. J. Neurosci. 28, 5229-5239.
1095 Dykes, I.M., Tempest, L., Lee, S.-I., Turner, E.E., 2011. Brn3a and Islet1 act epistatically to
1096 regulate the gene expression program of sensory differentiation. J. Neurosci. 31, 9789-
1097 9799.

1098 Eagleson, G.W., Dempewolf, R.D., 2002. The role of the anterior neural ridge and *Fgf-8* in
1099 early forebrain patterning and regionalization in *Xenopus laevis*. Comp. Biochem.
1100 Physiol. B Biochem. Mol. Biol. 132, 179-189.
1101 England, S.J., Cerda, G.A., Kowalchuk, A., Sorice, T., Grieb, G., Lewis, K.E., 2020. Hmx3a
1102 has essential functions in zebrafish spinal cord, ear and lateral line development.
1103 Genetics 216, 1153-1185.
1104 Fauber, B.P., Magnuson, S., 2014. Modulators of the nuclear receptor retinoic acid receptor-
1105 related orphan receptor-γ (RORγ or RORc). J. Med. Chem. 57, 5871-5892.
1106 Feng, Y., Xu, Q., 2010. Pivotal role of hmx2 and hmx3 in zebrafish inner ear and lateral line
1107 development. Dev. Biol. 339, 507-518.
1108 Freitas, R., Zhang, G., Albert, J.S., Evans, D.H., Cohn, M.J., 2006. Developmental origin of
1109 shark electrosensory organs. Evol. Dev. 8, 74-80.
1110 Gibbs, M.A., Northcutt, R.G., 2004a. Development of the lateral line system in the shovelnose
1111 sturgeon. Brain Behav. Evol. 64, 70-84.
1112 Gibbs, M.A., Northcutt, R.G., 2004b. Retinoic acid repatterns axolotl lateral line receptors. Int.
1113 J. Dev. Biol. 48, 63-66.
1114 Gillis, J.A., Modrell, M.S., Northcutt, R.G., Catania, K.C., Luer, C.A., Baker, C.V.H., 2012.
1115 Electrosensory ampullary organs are derived from lateral line placodes in cartilaginous
1116 fishes. Development 139, 3142-3146.
1117 Gnedeva, K., Hudspeth, A.J., 2015. SoxC transcription factors are essential for the
1118 development of the inner ear. Proc. Natl. Acad. Sci. U.S.A. 112, 14066-14071.
1119 Grabherr, M.G., Haas, B.J., Yassour, M., Levin, J.Z., Thompson, D.A., Amit, I., Adiconis, X.,
1120 Fan, L., Raychowdhury, R., Zeng, Q., Chen, Z., Mauceli, E., Hacohen, N., Gnirke, A.,
1121 Rhind, N., di Palma, F., Birren, B.W., Nusbaum, C., Lindblad-Toh, K., Friedman, N.,
1122 Regev, A., 2011. Full-length transcriptome assembly from RNA-Seq data without a
1123 reference genome. Nat. Biotechnol. 29, 644-652.
1124 Guindon, S., Dufayard, J.F., Lefort, V., Anisimova, M., Hordijk, W., Gascuel, O., 2010. New
1125 algorithms and methods to estimate maximum-likelihood phylogenies: assessing the
1126 performance of PhyML 3.0. Syst. Biol. 59, 307-321.
1127 Haber, A.L., Biton, M., Rogel, N., Herbst, R.H., Shekhar, K., Smillie, C., Burgin, G., Delorey,
1128 T.M., Howitt, M.R., Katz, Y., Tirosh, I., Beyaz, S., Dionne, D., Zhang, M., Raychowdhury,
1129 R., Garrett, W.S., Rozenblatt-Rosen, O., Shi, H.N., Yilmaz, O., Xavier, R.J., Regev, A.,
1130 2017. A single-cell survey of the small intestinal epithelium. Nature 551, 333-339.
1131 Hesse, K., Vaupel, K., Kurt, S., Buettner, R., Kirfel, J., Moser, M., 2011. AP-2δ is a crucial
1132 transcriptional regulator of the posterior midbrain. PLoS ONE 6, e23483.

1133 Hoffman, B.U., Baba, Y., Griffith, T.N., Mosharov, E.V., Woo, S.H., Roybal, D.D., Karsenty,
1134 G., Patapoutian, A., Sulzer, D., Lumpkin, E.A., 2018. Merkel cells activate sensory neural
1135 pathways through adrenergic synapses. Neuron 100, 1401-1413.e6.
1136 Houweling, A.C., Dildrop, R., Peters, T., Mummenhoff, J., Moorman, A.F.M., Rüther, U.,
1137 Christoffels, V.M., 2001. Gene and cluster-specific expression of the *Iroquois* family
1138 members during mouse development. Mech. Dev. 107, 169-174.
1139 Hu, X., Wang, Y., Hao, L.-Y., Liu, X., Lesch, C.A., Sanchez, B.M., Wendling, J.M., Morgan,
1140 R.W., Aicher, T.D., Carter, L.L., Toogood, P.L., Glick, G.D., 2015. Sterol metabolism
1141 controls T(H)17 differentiation by generating endogenous RORγ agonists. Nat. Chem.
1142 Biol. 11, 141-147.
1143 Huang, X., Chen, Q., Luo, W., Pakvasa, M., Zhang, Y., Zheng, L., Li, S., Yang, Z., Zeng, H.,
1144 Liang, F., Zhang, F., Hu, D.A., Qin, K.H., Wang, E.J., Qin, D.S., Reid, R.R., He, T.-C.,
1145 Athiviraham, A., El Dafrawy, M., Zhang, H., 2022. SATB2: A versatile transcriptional
1146 regulator of craniofacial and skeleton development, neurogenesis and tumorigenesis,
1147 and its applications in regenerative medicine. Genes Dis. 9, 95-107.
1148 Hwang, C.H., Simeone, A., Lai, E., Wu, D.K., 2009. *Foxg1* is required for proper separation
1149 and formation of sensory cristae during inner ear development. Dev. Dyn. 238, 2725-
1150 2734.
1151 Iyer, A.A., Groves, A.K., 2021. Transcription factor reprogramming in the inner ear: turning on
1152 cell fate switches to regenerate sensory hair cells. Front. Cell. Neurosci. 15, 660748.
1153 Iyer, A.A., Hosamani, I., Nguyen, J.D., Cai, T., Singh, S., McGovern, M.M., Beyer, L., Zhang,
1154 H., Jen, H.I., Yousaf, R., Birol, O., Sun, J.J., Ray, R.S., Raphael, Y., Segil, N., Groves,
1155 A.K., 2022. Cellular reprogramming with ATOH1, GFI1, and POU4F3 implicate
1156 epigenetic changes and cell-cell signaling as obstacles to hair cell regeneration in
1157 mature mammals. eLife 11, e79712.
1158 Jan, T.A., Eltawil, Y., Ling, A.H., Chen, L., Ellwanger, D.C., Heller, S., Cheng, A.G., 2021.
1159 Spatiotemporal dynamics of inner ear sensory and non-sensory cells revealed by single-
1160 cell transcriptomics. Cell Rep. 36, 109358.
1161 Jen, H.-I., Singh, S., Tao, L., Maunsell, H.R., Segil, N., Groves, A.K., 2022. GFI1 regulates
1162 hair cell differentiation by acting as an off-DNA transcriptional co-activator of ATOH1,
1163 and a DNA-binding repressor. Sci. Rep. 12, 7793.
1164 Jessen, K.R., Mirsky, R., 2019. Schwann cell precursors; multipotent glial cells in embryonic
1165 nerves. Front. Mol. Neurosci. 12, 69.
1166 Jørgensen, J.M., 2005. Morphology of electroreceptive sensory organs, in: T.H. Bullock, C.D.
1167 Hopkins, A.N. Popper, R.R. Fay (Eds.), Electroreception. Springer, New York, pp. 47-
1168 67.

1169 Kawauchi, S., Santos, R., Kim, J., Hollenbeck, P.L.W., Murray, R.C., Calof, A.L., 2009. The
1170 role of *Foxg1* in the development of neural stem cells of the olfactory epithelium. Ann.
1171 N. Y. Acad. Sci. 1170, 21-27.
1172 Kennedy, M.W., Chalamalasetty, R.B., Thomas, S., Garriock, R.J., Jailwala, P., Yamaguchi,
1173 T.P., 2016. Sp5 and Sp8 recruit β-catenin and Tcf1-Lef1 to select enhancers to activate
1174 Wnt target gene transcription. Proc. Natl. Acad. Sci. U.S.A. 113, 3545-3550.
1175 Kiernan, A.E., Pelling, A.L., Leung, K.K., Tang, A.S., Bell, D.M., Tease, C., Lovell-Badge, R.,
1176 Steel, K.P., Cheah, K.S., 2005. *Sox2* is required for sensory organ development in the
1177 mammalian inner ear. Nature 434, 1031-1035.
1178 Kotas, M.E., O'Leary, C.E., Locksley, R.M., 2023. Tuft cells: context- and tissue-specific
1179 programming for a conserved cell lineage. Annu. Rev. Pathol. 18, 311-335.
1180 Koth, M.L., Garcia-Moreno, S.A., Novak, A., Holthusen, K.A., Kothandapani, A., Jiang, K.,
1181 Taketo, M.M., Nicol, B., Yao, H.H.-C., Futtner, C.R., Maatouk, D.M., Jorgensen, J.S.,
1182 2020. Canonical Wnt/β-catenin activity and differential epigenetic marks direct sexually
1183 dimorphic regulation of *Irx3* and *Irx5* in developing mouse gonads. Development 147,
1184 dev183814.
1185 Ladurner, A., Schwarz, P.F., Dirsch, V.M., 2021. Natural products as modulators of retinoic
1186 acid receptor-related orphan receptors (RORs). Nat. Prod. Rep. 38, 757-781.
1187 Lecaudey, V., Anselme, I., Dildrop, R., Rüther, U., Schneider-Maunoury, S., 2005. Expression
1188 of the zebrafish Iroquois genes during early nervous system formation and patterning. J.
1189 Comp. Neurol. 492, 289-302.
1190 Leitch, D.B., Julius, D., 2019. Electrosensory transduction: comparisons across structure,
1191 afferent response properties, and cellular physiology., in: B.A. Carlson, J.A. Sisneros,
1192 A.N. Popper, R.R. Fay (Eds.), Electroreception: Fundamental Insights from Comparative
1193 Approaches. Springer, Cham, pp. 63-90.
1194 Lesko, M.H., Driskell, R.R., Kretzschmar, K., Goldie, S.J., Watt, F.M., 2013. Sox2 modulates
1195 the function of two distinct cell lineages in mouse skin. Dev. Biol. 382, 15-26.
1196 Li, X., Gaillard, F., Monckton, E.A., Glubrecht, D.D., Persad, A.R., Moser, M., Sauvé, Y.,
1197 Godbout, R., 2016. Loss of AP-2delta reduces retinal ganglion cell numbers and axonal
1198 projections to the superior colliculus. Mol. Brain 9, 62.
1199 Liang, J., Chirikjian, M., Pajvani, U.B., Bartolomé, A., 2022. MafA Regulation in β-Cells: From
1200 Transcriptional to Post-Translational Mechanisms. Biomolecules 12, 535.
1201 Lu, X., Sipe, C.W., 2016. Developmental regulation of planar cell polarity and hair-bundle
1202 morphogenesis in auditory hair cells: lessons from human and mouse genetics. WIREs
1203 Dev. Biol. 5, 85-101.
1204 Lush, M.E., Diaz, D.C., Koenecke, N., Baek, S., Boldt, H., St Peter, M.K., Gaitan-Escudero,
1205 T., Romero-Carvajal, A., Busch-Nentwich, E.M., Perera, A.G., Hall, K.E., Peak, A., Haug,

1206 J.S., Piotrowski, T., 2019. scRNA-Seq reveals distinct stem cell populations that drive
1207 hair cell regeneration after loss of Fgf and Notch signaling. eLife 8, e44431.
1208 Mak, A.C.Y., Szeto, I.Y.Y., Fritzsch, B., Cheah, K.S.E., 2009. Differential and overlapping
1209 expression pattern of SOX2 and SOX9 in inner ear development. Gene Expr. Patterns
1210 9, 444-453.
1211 Martik, M.L., Gandhi, S., Uy, B.R., Gillis, J.A., Green, S.A., Simoes-Costa, M., Bronner, M.E.,
1212 2019. Evolution of the new head by gradual acquisition of neural crest regulatory circuits.
1213 Nature 574, 675-678.
1214 Matern, M.S., Milon, B., Lipford, E.L., McMurray, M., Ogawa, Y., Tkaczuk, A., Song, Y., Elkon,
1215 R., Hertzano, R., 2020. GFI1 functions to repress neuronal gene expression in the
1216 developing inner ear hair cells. Development 147, dev186015.
1217 McGinnis, S., Madden, T.L., 2004. BLAST: at the core of a powerful and diverse set of
1218 sequence analysis tools. Nucleic Acids Res. 32, W20-5.
1219 Meijer, F.A., Doveston, R.G., de Vries, R.M.J.M., Vos, G.M., Vos, A.A.A., Leysen, S.,
1220 Scheepstra, M., Ottmann, C., Milroy, L.-G., Brunsveld, L., 2020. Ligand-based design of
1221 allosteric retinoic acid receptor-related orphan receptor γt (RORγt) inverse agonists. J.
1222 Med. Chem. 63, 241-259.
1223 Metscher, B.D., Müller, G.B., 2011. MicroCT for molecular imaging: quantitative visualization
1224 of complete three-dimensional distributions of gene products in embryonic limbs. Dev.
1225 Dyn. 240, 2301-2308.
1226 Miller, S.R., Perera, S.N., Baker, C.V.H., 2017. Constitutively active Notch1 converts cranial
1227 neural crest-derived frontonasal mesenchyme to perivascular cells *in vivo*. Biol. Open 6,
1228 317-325.
1229 Modrell, M.S., Baker, C.V.H., 2012. Evolution of electrosensory ampullary organs:
1230 conservation of *Eya4* expression during lateral line development in jawed vertebrates.
1231 Evol. Dev. 14, 277-285.
1232 Modrell, M.S., Bemis, W.E., Northcutt, R.G., Davis, M.C., Baker, C.V.H., 2011a.
1233 Electrosensory ampullary organs are derived from lateral line placodes in bony fishes.
1234 Nat. Commun. 2, 496.
1235 Modrell, M.S., Buckley, D., Baker, C.V.H., 2011b. Molecular analysis of neurogenic placode
1236 development in a basal ray-finned fish. genesis 49, 278-294.
1237 Modrell, M.S., Lyne, M., Carr, A.R., Zakon, H.H., Buckley, D., Campbell, A.S., Davis, M.C.,
1238 Micklem, G., Baker, C.V.H., 2017a. Insights into electrosensory organ development,
1239 physiology and evolution from a lateral line-enriched transcriptome. eLife 6, e24197.
1240 Modrell, M.S., Tidswell, O.R.A., Baker, C.V.H., 2017b. Notch and Fgf signaling during
1241 electrosensory versus mechanosensory lateral line organ development in a non-teleost
1242 ray-finned fish. Dev. Biol. 431, 48-58.

1243 Mogdans, J., 2019. Sensory ecology of the fish lateral-line system: Morphological and
1244 physiological adaptations for the perception of hydrodynamic stimuli. J. Fish Biol. 95, 53-
1245 72.
1246 Moser, T., Grabner, C.P., Schmitz, F., 2020. Sensory processing at ribbon synapses in the
1247 retina and the cochlea. Physiol. Rev. 100, 103-144.
1248 Norris, H.W., Hughes, S.P., 1920. The spiracular sense-organ in elasmobranchs, ganoids and
1249 dipnoans. Anat. Rec. 18, 205-209.
1250 Northcutt, R.G., 1997. Evolution of gnathostome lateral line ontogenies. Brain Behav. Evol.
1251 50, 25-37.
1252 Northcutt, R.G., Brändle, K., Fritzsch, B., 1995. Electroreceptors and mechanosensory lateral
1253 line organs arise from single placodes in axolotls. Dev. Biol. 168, 358-373.
1254 Ó Maoiléidigh, D., Ricci, A.J., 2019. A bundle of mechanisms: inner-ear hair-cell
1255 mechanotransduction. Trends Neurosci. 42, 221-236.
1256 O'Donnell, M., Hong, C.-S., Huang, X., Delnicki, R.J., Saint-Jeannet, J.-P., 2006. Functional
1257 analysis of Sox8 during neural crest development in *Xenopus*. Development 133, 3817-
1258 3826.
1259 O'Neill, P., McCole, R.B., Baker, C.V.H., 2007. A molecular analysis of neurogenic placode
1260 and cranial sensory ganglion development in the shark, *Scyliorhinus canicula*. Dev. Biol.
1261 304, 156-181.
1262 Pangrsic, T., Singer, J.H., Koschak, A., 2018. Voltage-gated calcium channels: key players in
1263 sensory coding in the retina and the inner ear. Physiol Rev. 98, 2063-2096.
1264 Papalopulu, N., Kintner, C., 1996. A posteriorising factor, retinoic acid, reveals that
1265 anteroposterior patterning controls the timing of neuronal differentiation in *Xenopus*
1266 neuroectoderm. Development 122, 3409-3418.
1267 Pauley, S., Lai, E., Fritzsch, B., 2006. *Foxg1* is required for morphogenesis and histogenesis
1268 of the mammalian inner ear. Dev. Dyn. 235, 2470-2482.
1269 Perdigoto, C.N., Bardot, E.S., Valdes, V.J., Santoriello, F.J., Ezhkova, E., 2014. Embryonic
1270 maturation of epidermal Merkel cells is controlled by a redundant transcription factor
1271 network. Development 141, 4690-4696.
1272 Piotrowski, T., Baker, C.V.H., 2014. The development of lateral line placodes: Taking a
1273 broader view. Dev. Biol. 389, 68-81.
1274 Reilly, M.B., Cros, C., Varol, E., Yemini, E., Hobert, O., 2020. Unique homeobox codes
1275 delineate all the neuron classes of *C. elegans*. Nature 584, 595-601.
1276 Roccio, M., Senn, P., Heller, S., 2020. Novel insights into inner ear development and
1277 regeneration for targeted hearing loss therapies. Hear. Res. 397, 107859.

1278 Romero-Carvajal, A., Navajas Acedo, J., Jiang, L., Kozlovskaja-Gumbriene, A., Alexander, R.,
1279 Li, H., Piotrowski, T., 2015. Regeneration of sensory hair cells requires localized
1280 interactions between the Notch and Wnt pathways. Dev. Cell 34, 267-282.
1281 Saito, T., Psenicka, M., 2015. Novel technique for visualizing primordial germ cells in
1282 sturgeons (*Acipenser ruthenus*, *A. gueldenstaedtii*, *A. baerii*, and *Huso huso*). Biol.
1283 Reprod. 93, 96.
1284 Sapède, D., Gompel, N., Dambly-Chaudière, C., Ghysen, A., 2002. Cell migration in the
1285 postembryonic development of the fish lateral line. Development 129, 605-615.
1286 Schulz, M.H., Zerbino, D.R., Vingron, M., Birney, E., 2012. Oases: robust *de novo* RNA-seq
1287 assembly across the dynamic range of expression levels. Bioinformatics 28, 1086-1092.
1288 Stehlin-Gaon, C., Willmann, D., Zeyer, D., Sanglier, S., Van Dorsselaer, A., Renaud, J.-P.,
1289 Moras, D., Schüle, R., 2003. All-*trans* retinoic acid is a ligand for the orphan nuclear
1290 receptor ROR beta. Nat. Struct. Biol. 10, 820-825.
1291 Stundl, J., Pospisilova, A., Matějková, T., Psenicka, M., Bronner, M.E., Cerny, R., 2020.
1292 Migratory patterns and evolutionary plasticity of cranial neural crest cells in ray-finned
1293 fishes. Dev. Biol. 467, 14-29.
1294 Stundl, J., Soukup, V., Franěk, R., Pospisilova, A., Psutkova, V., Pšenička, M., Cerny, R.,
1295 Bronner, M.E., Medeiros, D.M., Jandzik, D., 2022. Efficient CRISPR mutagenesis in
1296 sturgeon demonstrates its utility in large, slow-maturing vertebrates. Front. Cell Dev.
1297 Biol. 10, 750833.
1298 Sun, Y., Dykes, I.M., Liang, X., Eng, S.R., Evans, S.M., Turner, E.E., 2008. A central role for
1299 Islet1 in sensory neuron development linking sensory and spinal gene regulatory
1300 programs. Nat. Neurosci. 11, 1283-1293.
1301 Tasdemir-Yilmaz, O.E., Druckenbrod, N.R., Olukoya, O.O., Dong, W., Yung, A.R., Bastille, I.,
1302 Pazyra-Murphy, M.F., Sitko, A.A., Hale, E.B., Vigneau, S., Gimelbrant, A.A.,
1303 Kharchenko, P.V., Goodrich, L.V., Segal, R.A., 2021. Diversity of developing peripheral
1304 glia revealed by single-cell RNA sequencing. Dev. Cell 56, 2516-2535.
1305 Toresson, H., Martinez-Barbera, J.P., Bardsley, A., Caubit, X., Krauss, S., 1998. Conservation
1306 of *BF-1* expression in amphioxus and zebrafish suggests evolutionary ancestry of
1307 anterior cell types that contribute to the vertebrate telencephalon. Dev. Genes Evol. 208,
1308 431-439.
1309 Undurraga, C.A., Gou, Y., Sandoval, P.C., Nuñez, V.A., Allende, M.L., Riley, B.B., Hernández,
1310 P.P., Sarrazin, A.F., 2019. Sox2 and Sox3 are essential for development and
1311 regeneration of the zebrafish lateral line. bioRxiv 856088; doi:
1312 https://doi.org/10.1101/856088.
1313 UniProt, Consortium, 2023. UniProt: the Universal Protein Knowledgebase in 2023. Nucleic
1314 Acids Res. 51, D523-D531.

1315 Vidal, B., Gulez, B., Cao, W.X., Leyva-Díaz, E., Reilly, M.B., Tekieli, T., Hobert, O., 2022. The
1316 enteric nervous system of the *C. elegans* pharynx is specified by the Sine oculis-like
1317 homeobox gene *ceh-34*. eLife 11, e76003.
1318 von Bartheld, C.S., Giannessi, F., 2011. The paratympanic organ: a barometer and altimeter
1319 in the middle ear of birds? J. Exp. Zool. B Mol. Dev. Evol. 316, 402-408.
1320 Wang, J., Lu, C., Zhao, Y., Tang, Z., Song, J., Fan, C., 2020. Transcriptome profiles of
1321 sturgeon lateral line electroreceptor and mechanoreceptor during regeneration. BMC
1322 Genomics 21, 875.
1323 Webb, J.F., 2021. Morphology of the mechanosensory lateral line system of fishes, in: B.
1324 Fritzsch (Ed.), The Senses: A Comprehensive Reference. Elsevier, pp. 29-46.
1325 Wiwatpanit, T., Lorenzen, S.M., Cantú, J.A., Foo, C.Z., Hogan, A.K., Márquez, F., Clancy,
1326 J.C., Schipma, M.J., Cheatham, M.A., Duggan, A., García-Añoveros, J., 2018. Trans-
1327 differentiation of outer hair cells into inner hair cells in the absence of INSM1. Nature
1328 563, 691-695.
1329 Yamashita, T., Zheng, F., Finkelstein, D., Kellard, Z., Robert, C., Rosencrance, C.D., Sugino,
1330 K., Easton, J., Gawad, C., Zuo, J., 2018. High-resolution transcriptional dissection of *in*
1331 *vivo* Atoh1-mediated hair cell conversion in mature cochleae identifies Isl1 as a co-
1332 reprogramming factor. PLoS Genet. 14, e1007552.
1333 Zeiske, E., Kasumyan, A., Bartsch, P., Hansen, A., 2003. Early development of the olfactory
1334 organ in sturgeons of the genus *Acipenser*: a comparative and electron microscopic
1335 study. Anat. Embryol. (Berl.) 206, 357-372.
1336 Zerbino, D.R., Birney, E., 2008. Velvet: algorithms for de novo short read assembly using de
1337 Bruijn graphs. Genome Res. 18, 821-829.
1338 Zhang, S., Zhang, Y., Dong, Y., Guo, L., Zhang, Z., Shao, B., Qi, J., Zhou, H., Zhu, W., Yan,
1339 X., Hong, G., Zhang, L., Zhang, X., Tang, M., Zhao, C., Gao, X., Chai, R., 2019.
1340 Knockdown of *Foxg1* in supporting cells increases the trans-differentiation of supporting
1341 cells into hair cells in the neonatal mouse cochlea. Cell. Mol. Life Sci. 77, 1401-1419.
1342 Zhang, Y., Zhang, S., Zhang, Z., Dong, Y., Ma, X., Qiang, R., Chen, Y., Gao, X., Zhao, C.,
1343 Chen, F., He, S., Chai, R., 2020. Knockdown of *Foxg1* in Sox9+ supporting cells
1344 increases the trans-differentiation of supporting cells into hair cells in the neonatal mouse
1345 utricle. Aging (Albany NY) 12, 19834-19851.
1346 Zhao, X.-F., Suh, C.S., Prat, C.R., Ellingsen, S., Fjose, A., 2009. Distinct expression of two
1347 *foxg1* paralogues in zebrafish. Gene Expr. Patterns 9, 266-272.
1348

1349

Expressed in ampullary organs and neuromasts	Electrosensory-restricted	Mechanosensory-restricted
Atoh1 [3,4]	*Insm1*	*Foxg1*
Elf3	*Irx5*	*Hmx2*
Eya1 [1]	*Mafa*	*Isl1*
Eya2 [1]	*Neurod4* [4]	*Rorb*
Eya3 [1]	*Rorc*	*Sox8*
Eya4 [1]	*Satb2*	
Gfi1	*Sp5*	
Hes5 [5]		
Hey2		
Insm2		
Irx1		
Klf17		
Lhx3 [4]		
Lhx6-like		
Myt1 [4]		
Otx1		
Pou4f1 [4]		
Pou4f3 [4]		
Six1 [1]		
Six2 [1]		
Six4 [1]		
Sox1 [4]		
Sox2 [4]		
Sox3 [1]		
Sox4		
Sox9		
Tfap2d		
Znf703		

1350

1351 **Table 1. Transcription factor genes expressed in developing lateral line organs in**
1352 **paddlefish and/or sterlet.** Lateral line expression was reported either in this study or in
1353 previous papers, denoted by numbers in brackets: [1] Modrell et al. (2011b); [2] Modrell et al.
1354 (2011a); [3] Butts et al. (2014); [4] Modrell et al. (2017a); [5] Modrell et al. (2017b).